Received: 27 April 2022 | Revised: 14 October 2022 | Accepted: 17 October 2022

DOI: 10.1111/mec.16760

ORIGINAL ARTICLE

MOLECULAR ECOLOGY WILEY

Transitioning from microsatellites to SNP-based microhaplotypes in genetic monitoring programmes: Lessons from paired data spanning 20 years

Megan J. Osborne | Guilherme Caeiro-Dias | Thomas F. Turner

Department of Biology and Museum of Southwestern Biology, University of New Mexico, Albuquerque, New Mexico, USA

Correspondence
Megan J. Osborne, Department of Biology and Museum of Southwestern Biology, MSC 03-2020, University of New Mexico, Albuquerque, NM 87131, USA.
Email: mosborne@unm.edu

Funding information
U.S. Bureau of Reclamation, Grant/Award Number: R18AP00130

Handling Editor: Paul A. Hohenlohe

Abstract

Many long-term genetic monitoring programmes began before next-generation sequencing became widely available. Older programmes can now transition to new marker systems usually consisting of 1000s of SNP loci, but there are still important questions about comparability, precision, and accuracy of key metrics estimated using SNPs. Ideally, transitioned programmes should capitalize on new information without sacrificing continuity of inference across the time series. We combined existing microsatellite-based genetic monitoring information with SNP-based microhaplotypes obtained from archived samples of Rio Grande silvery minnow (*Hybognathus amarus*) across a 20-year time series to evaluate point estimates and trajectories of key genetic metrics. Demographic and genetic monitoring bracketed multiple collapses of the wild population and included cases where captive-born repatriates comprised the majority of spawners in the wild. Even with smaller sample sizes, microhaplotypes yielded comparable and in some cases more precise estimates of variance genetic effective population size, multilocus heterozygosity and inbreeding compared to microsatellites because many more microhaplotype loci were available. Microhaplotypes also recorded shifts in allele frequencies associated with population bottlenecks. Trends in microhaplotype-based inbreeding metrics were associated with the fraction of hatchery-reared repatriates to the wild and should be incorporated into future genomic monitoring. Although differences in accuracy and precision of some metrics were observed between marker types, biological inferences and management recommendations were consistent.

KEYWORDS
demography, genetic effective population size, inbreeding, long-term monitoring, multilocus heterozygosity, RAD-seq, rapid evolution

1 | INTRODUCTION

Genetic monitoring quantifies trajectories of individual- and population-level metrics that include heterozygosity, gene diversity and genetic effective population size (N_e) over contemporary time series (Schwartz et al., 2007). Tracking these metrics facilitates adaptive and evolutionary-cognizant management. For the past three decades, microsatellites were the workhorse for genetic monitoring programmes (e.g., Beatty et al., 2014; Dowling et al., 2014; Koelewijn et al., 2010). Long-term monitoring programmes are now transitioning to next-generation high-throughput genomic approaches based on single-nucleotide polymorphisms (SNPs) and microhaplotypes (i.e., multiple SNPs haplotyped at the same locus); raising questions about continuity and consistency across the time series as well as

the relative accuracy, precision and comparability of metrics estimated with different genetic marker classes. The transition process also offers opportunities to adjust metrics and analytical procedures to better capitalize on whole-genome screening, preferably without loss of information. Microsatellite panels typically represent few loci and a small fraction of the genome, but often exhibit high rates of evolution and many distinct alleles per locus. High-throughput protocols generate SNP data sets that include numerous loci (often >1000) that are widespread throughout the genome, but possible allelic states at each locus is limited. Next-generation sequencing typically identifies multiple SNPs on a single DNA fragment but to avoid issues with linkage, only a single SNP per fragment is retained (O'Leary et al., 2021). However, SNPs found on the same fragment can be kept as multiallelic microhaplotypes to increase power for estimating key metrics (Baetscher et al., 2018). Increased power may be especially important for rare and endangered species with depleted genetic variation. What do differences between marker types portend for comparative inferential power and, in the case of conserved populations, recommendations based on monitoring made to resource managers?

Performance of microsatellites and other types of markers (biallelic SNPs, microhaplotypes) has been evaluated in the context of spatial patterns of genetic variation, for a variety of organisms, for example, threespine stickleback (*Gasterosteus aculeatus*; DeFaveri et al., 2013), bighorn sheep (*Ovis canadensis*; Miller et al., 2014), brown trout (*Salmo trutta*; Lemopoulos et al., 2019), northern pike (*Esox lucius*; Sunde et al., 2020) and walleye (*Sander vitreus*; Bootsma et al., 2021). The consensus is that marker types recovered similar patterns of broad-scale population structure, but the relative performance of different marker types is context dependent (i.e., number of loci, alleles, etc.). We are not aware of any study that explicitly compares key metrics across marker types over time to evaluate trends in genetic diversity and effective size, even though temporal studies are the foundation of genetic monitoring.

At the individual-level, some studies reported weak correlations of estimates obtained from microsatellite and SNP data across metrics of relatedness, individual-level heterozygosity, parentage, and population diversity (e.g., DeFaveri et al., 2013; Fischer et al., 2017). In most cases, this is attributed to heterogeneity across the genome that may weaken correlations between markers. Chakraborty (1981) showed that individual heterozygosity estimated from a small number of molecular markers does not adequately represent genome-wide heterozygosity (GWH) especially in the absence of identity disequilibrium (ID, i.e., nonrandom associations of genotypes between loci; DeWoody & DeWoody, 2005; Ljungqvist et al., 2010). For correlations between genome-wide heterozygosity and diversity, populations must display ID (Ljungqvist et al., 2010), without which, all loci within the genome will be heterozygous or homozygous independently of each other (Szulkin et al., 2010). Identity disequilibrium occurs when there are some consanguineous matings in the population (Bennett & Binet, 1956; Ohta & Cockerham, 1974) and ID can be used as a proxy for inbreeding (Miller et al., 2014). Population bottlenecks and genetic drift, as a cause and consequence of small population size, lead to matings between related individuals resulting in ID. Likewise, admixture can result in temporary ID because individuals with ancestors from divergent populations are outbred, relative to individuals originating from a shared ancestral population.

Importantly, genetic monitoring potentially provides real-time insight into the relationship between heterozygosity and fitness (i.e., heterozygosity fitness correlation [HFC]), including variation in reproductive success. Within populations, variation in inbreeding affects genome-wide genotypic variation among individuals and causes subsequent fitness differences among them (Sin et al., 2021). Studies measuring HFC are conducted to detect evidence of inbreeding depression which can compromise population viability and conservation efforts (e.g., Hoffman et al., 2014; Townsend & Jamieson, 2013). Until recently, microsatellites were the marker of choice for genetic monitoring and HFC studies due to their high variability and minimal development costs. However, ascertainment bias caused by selecting only the most polymorphic microsatellite loci results in reduced sensitivity for assessing genome-wide genetic diversity (Väli et al., 2008) while the small number of microsatellite loci typically employed limits power to detect inbreeding (Szulkin et al., 2010). Furthermore, estimates of inbreeding and individual heterozygosity obtained from few loci are poorly correlated under most realistic situations (Balloux et al., 2004; Miller & Coltman, 2014). Moreover, microsatellite data sets are often replete with missing data, null alleles and scoring errors that impact some population-level metrics, most notably F_{IS} (e.g., David et al., 2007) and genetic effective population size (Marandel et al., 2020). SNPs appear to improve accuracy and precision of GWH estimates and inbreeding (Hoffman et al., 2014; Sin et al., 2021). Yet, although there are numerous molecular-based surrogates for inbreeding (e.g., realized individual inbreeding [F], internal relatedness [IR], multilocus heterozygosity [MLH] and g_2; Table 1), these are not typically measured in genetic monitoring programmes. As monitoring programmes begin to transition toward genomic scale data, uncertainties remain regarding the utility of these alternate statistics related to inbreeding.

Simulation studies offer some guidance on the comparative sensitivity of microsatellites and biallelic SNPs to detect population declines over time, and under different demographic scenarios and sampling schemes at conservation-relevant timescales (Hoban et al., 2014). Data from real populations are scarce (but see Lehnert et al., 2018) and the relative power of microhaplotypes has not been investigated to our knowledge. A long-term genetic and demographic monitoring programme of the Rio Grande silvery minnow (*Hybognathus amarus*) provides an opportunity to conduct a side-by-side comparison between microsatellites and microhaplotypes obtained from representative archived samples. Over the last 70 years, this species has contended with habitat changes associated with river fragmentation, dewatering, and flood control that have caused significant range contraction (Platania, 1993). Since listing under the Endangered Species Act in 1994 (U.S. Fish and Wildlife Service, 1994), droughts and water extraction have caused periodic population collapses associated with recruitment failure (Archdeacon et al., 2020; Archdeacon & Reale, 2020). A

TABLE 1 Description of statistics used to measure inbreeding/identity disequilibrium

Symbol	Statistic	Description	Reference
$\hat{g}_2$	Identity disequilibrium	• Low-bias estimate of g_2. Measures excess of double heterozygotes at two loci relative to expectations (equation 8 in David et al., 2007)	David et al. (2007)
sMLH	Standardized multilocus heterozygosity	• Mean heterozygosity across all genotyped loci divided by mean heterozygosity at loci genotyped in the population (i.e., temporal sample). Standardizes heterozygosity when not all loci are typed in each individual	Coltman et al. (1999)
IR	Internal relatedness	• IR = $(2H - \sum fi) / (2N - \sum fi)$ where H is the number of homozygous loci and N is the number if loci and fi is the frequency of the ith allele in the genotype. Weights rare alleles more heavily	Amos et al. (2001)
F_{IS}	Fixation index	• Inbreeding at the population level with respect to nonrandom mating within demes. Measures heterozygote deficiency/excess per locus. $F_{IS} = \frac{H_{exp} - H_{obs}}{H_{exp}}$	Wright (1950)
F	IBD inbreeding	• F calculated by EMIBD is derived from estimates of the 9 condensed IBD coefficients between two individuals. $\overline{F}$ is the average F for each individual. $\overline{F}_{pop}$-population average	Wang (2021)

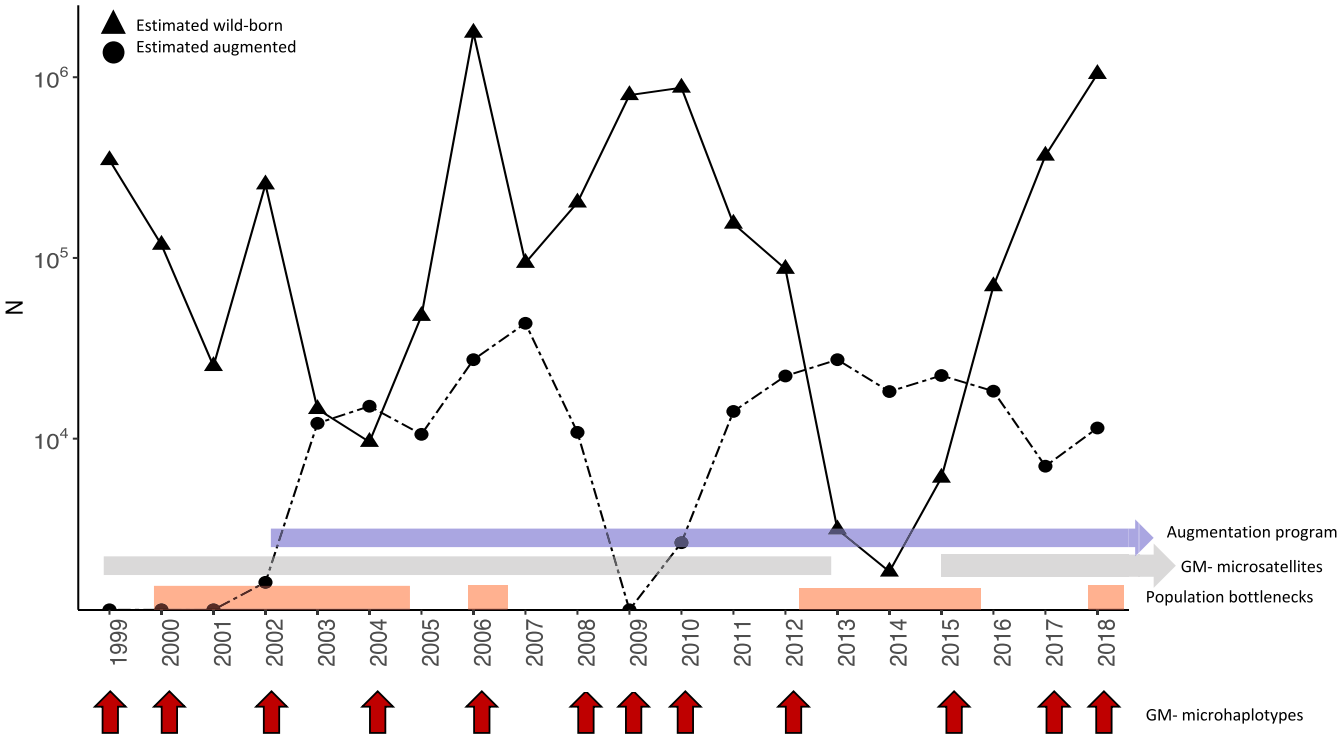

FIGURE 1 Summary of the of the main demographic events and management actions since the beginning of genetic monitoring of Rio Grande silvery minnow. This species was listed under the endangered species act in 1994. Genetic monitoring (GM) commenced in 1999 and has continued annually since (except for 2013–2014 when insufficient samples were available for genetic analysis). A captive breeding and rearing programme commenced on a limited scale in 2002 and in 2003, transitioned to a full-scale programme with the founding of the captive population from 922,000 eggs from natural reproduction of the middle Rio Grande population (indicated by the purple arrow). The population has been augmented nearly every year since. Samples used for SNP discovery are indicated by the red arrows. Population bottlenecks are indicated by the red bars. N-estimated wild-born and augmented Rio Grande silvery minnow from Yackulic et al. (2022)

full-scale captive breeding and augmentation programme began in 2002–2003 (U.S. Fish and Wildlife Service, 2018a, 2018b) and progeny from this programme sometimes comprise the majority of the spawning stock in the wild. Population bottlenecks and genetic drift associated with augmentation are expected to impact GWH (Szulkin et al., 2010) and genetic monitoring of the population should reveal signatures of these events in the genome provided genetic markers have sufficient power.

Like other conservation programmes, maintenance of genome-wide diversity and adaptive potential are major tenets of the Rio Grande silvery minnow conservation programme, but whether findings from small panels of microsatellites accurately reflect genome-wide patterns have been widely debated (e.g., Miller et al., 2014). Results obtained from microhaplotypes also must be directly comparable to previous results to preserve the continuity and comparability of the time series. Using a genetic monitoring time series spanning two decades we: (1) summarized patterns of genetic variation, divergence and effective size using microsatellites and microhaplotypes; (2) assessed whether measures of population genetic diversity, individual diversity, divergence and contemporary genetic effective population size were correlated between microsatellites and microhaplotypes; and (3) assessed whether other metrics (i.e., MLH, IR, g_2) estimated from genomic data, would be a valuable addition to genetic monitoring programmes. Leveraging the power of genomic data could provide additional insight not afforded by microsatellite markers, thereby strengthening the value of genetic monitoring to ongoing adaptive management of the species.

2 | MATERIALS AND METHODS

2.1 | Demographic monitoring data and modelling

Rio Grande silvery minnow is a small-bodied, short-lived cyprinid (Horwitz et al., 2018) that was widely distributed in the Rio Grande from northern New Mexico to the Gulf of Mexico, and in the Pecos River from northern New Mexico to the confluence of the Rio Grande in Texas (Pflieger, 1980). A remnant population persists in the Rio Grande in New Mexico extending from downstream of Cochiti Dam to Elephant Butte Reservoir (Bestgen & Platania, 1991). This river reach is referred to as the middle Rio Grande. Platania (1993) first documented the rapid decline of the species in the middle Rio Grande in the late 1980s. Since 1993, systematic demographic monitoring has been conducted from April to October at 20 localities encompassing the species current range, revealing recurrent order-of-magnitude declines in the population (e.g., Dudley et al., 2021). Population declines are typically associated with periods of reduced spring runoff and prolonged periods of low flow over the summer months (Archdeacon, 2016; Dudley et al., 2019; Figure 1). Conversely, periods of elevated and protracted spring flows and limited summer drying are associated with increased abundance. Periods of greatly reduced densities (<1 fish per 100 m^2) were documented between 2000–2004, 2006, 2012–2015 and in 2018 (Dudley et al., 2019) while 1996, 2010 and 2011 were only marginally better (1–2 fish per 100 m^2). Highest densities were recorded in 1995, 2005 and 2017 (estimated densities 23.17–44.85 fish per 100 m^2). These data confirm that declines can be precipitous from one year to the next, and that the species has the capacity to recover following periods of low abundance. Large-scale propagation began in 2002–2003 with annual spring collections of hundreds of thousands of eggs from riverine spawning. Eggs were reared in captivity and released as prereproductive adults the following winter. Incorporation of eggs produced from riverine spawning into hatchery activities, captive spawning of wild-origin individuals, and annual augmentation are now cornerstones of recovery efforts for the species (U.S. Fish and Wildlife Service, 2018a). Genetic monitoring began in 1999 and is conducted annually using microsatellites and mitochondrial DNA markers (Osborne et al., 2012). Metrics tracked include standard diversity measures (Nei's unbiased gene diversity [uH_S], observed heterozygosity [H_O] and allelic richness [A_R]), variance genetically effective population size (N_{eV}), and linkage disequilibrium effective population size (N_{eD}).

To allow genetic data to be interpreted with reference to population demography, the number of wild-born and augmented fish in each year were estimated using a population model (Yackulic et al., 2022). The model integrates Rio Grande silvery minnow abundance estimates made from 2008 to 2011 (Dudley et al., 2012), with catch-per-unit-effort (CPUE) data collected monthly between April and November, along with estimates of habitat availability. Abundances were directly estimated by the model for each year between 2002 and 2018. Abundances for 1999 and 2000 were extrapolated by analysing observed river discharge and catch-per-unit-effort data in a Bayesian model that used parameter estimates and associated uncertainty to estimate prior distributions.

2.2 | Sample selection

Samples for SNP identification were selected from archived Rio Grande silvery minnow held at the Museum of Southwestern Biology, Division of Fishes. Samples were selected based on: (1) preservation method (frozen or 95% ethanol), (2) year of collection (the earliest ethanol/frozen material was collected in 1999), and (3) collection locality (Table S1). We selected samples that represented the temporal scale of ongoing genetic monitoring (1999–2018) and bracketed population bottlenecks identified from demographic monitoring (Figure 1). We included ~10 samples from each of three populated river reaches (Angostura, Isleta and San Acacia—when available) to reflect the spatial scale of monitoring, which encompasses the entire geographic range of the species. Population genetic analysis was based on total number of samples (pooled across reaches), since there is little evidence of population structure between reaches (Osborne et al., 2012). Additional samples were included from 1999 and 2000 to provide redundancy in the event of poor sample quality (i.e., degraded DNA) in older samples, and to obtain genomic data prior to the beginning of the conservation hatchery and augmentation programme. To ensure representative coverage of the time series (i.e., a sample every 2 years) we purified archived DNA (originally isolated using a proteinase-K and phenol-chloroform protocol) when tissue samples were not available (Table 2). A total of 379 samples were included for DNA sequencing. Sequence quality was assessed by preservation type using the nonparametric Kruskal-Wallis test implemented in the R package stats version 4.0.3 (details in Figure S1).

TABLE 2 Temporal and spatial origin of Rio Grande silvery minnow samples for SNP discovery

River reach	1999	2000	2002	2004	2006	2008	2009	2010	2012	2015	2017	2018
Angostura	–	–	9	10	10*	10*	10*	9*	10	11*	10*	10*
Isleta	–	–	11	10	10*	10*	–	10*	11	11*	10*	10*
San Acacia	30*	42*	10	6	10*	10*	20*	10*	9	9*	10*	20*
Total	30	42	30	28	30	30	30	29	30	31	30	40

Note: Asterisks denote tissue samples (frozen and ethanol). All other samples were purified from previous DNA isolations. The total number of samples was 379 (13 samples were later discarded because of missing data). Analyses were based on total number of samples per year, since there is no evidence of population structure between river reaches (Osborne et al., 2012).

2.3 | NextRAD sequencing

Isolation of DNA from tissue samples was performed using E.Z.N.A. tissue DNA (Omega Bio-Tek Inc.) or Zymo Quick-DNA (Zymo Research Corp) kits according to the procedures outlined by the manufacturer. Isolations of DNA from previous genetic monitoring were purified using Zymo DNA clean and concentrator kits to remove phenol which can inhibit DNA sequencing. All samples were treated with RNase A. Each isolate was evaluated for the presence of high molecular weight DNA and the absence of RNA contamination by electrophoresis on a 1.2% agarose gel. Double-stranded DNA was quantified using Qubit BR assays (Invitrogen, Thermo Fisher Scientific) and samples with sufficient high-quality DNA were submitted for sequencing at SNPsaurus, LLC (University of Oregon). Genomic DNA was converted into Nextera-tagmented reductively-amplified DNA genotyping-by-sequencing (nextRAD) libraries and sequenced according to Russello et al. (2015). Additional details are provided in the supplementary material. Genomic DNA fragments were pooled in two nextRAD libraries, each sequenced on two Illumina Hi-Seq 4000 lanes of 150 base pair (bp) single-end reads.

2.4 | Microsatellites

Microsatellite data from nine loci previously genotyped in samples spanning the period 1999–2010 (Osborne et al., 2012; Supporting Information) were used in this study for comparative analysis. In addition, microsatellite data was included from 1570 individuals collected as part of ongoing monitoring for 2012, 2015, 2017, and 2018 from the Rio Grande using methods described previously. Data from these additional years were paired directly with microhaplotype data.

2.5 | Variant calling and quality filtering

Raw DNA sequences obtained from nextRAD sequencing from 379 individuals were demultiplexed by sequencing lane and unique DNA barcode combinations that identified individuals. Raw reads were trimmed and aligned to a draft female Rio Grande silvery minnow reference genome. Resulting nextRAD loci were used to call variants that were subsequently filtered to obtain a biallelic SNP data set. Next, the variable positions in each locus were haplotyped (hereafter referred to as microhaplotypes) as described by Willis et al. (2017). Finally, we tested microhaplotypes for deviations from Hardy–Weinberg equilibrium (HWE) and in linkage disequilibrium (LD). A detailed description of the procedure, software, filters and options employed to obtain the final data set is presented in Table S2.

2.6 | Genetic diversity

We calculated the percentage of missing data (% MD) per individual and locus for both data sets using the program GenoDive (Meirmans, 2020). Large % MD affects estimation of some metrics (e.g., F_{IS} and N_e), adding uncertainty that confounds interpretation of downstream results (e.g., Marandel et al., 2020). We calculated standard genetic diversity metrics typically used in genetic monitoring programmes, including Nei's unbiased gene diversity (Nei, 1987) and heterozygosity for each temporal sample using the program GenoDive version 3.0 (Meirmans, 2020) to enable comparisons between marker types. Allelic richness and average inbreeding coefficients (F_{IS}) were calculated using the R package diveRsity version 1.9.90 (Keenan et al., 2013). The 95% confidence intervals (CIs) were calculated for uH_S, H_O and F_{IS}. For microsatellites, GenePop'007 (Rousset, 2008) was used to test for departures from Hardy–Weinberg equilibrium (HWE) using the procedure of Guo and Thompson (1992) and to perform global tests for linkage disequilibrium for all pairs of loci in each collection. Sequential Bonferroni correction (Rice, 1989) was applied to account for inflated type I error rates associated with multiple simultaneous tests. We used Pearson correlations to examine whether % MD was correlated with diversity metrics and to evaluate concordance between comparable metrics estimated from microsatellites and microhaplotypes.

2.7 | Genetic effective population size

The linkage disequilibrium method (Hill, 1981) was used to estimate the N_{eD} for each collection of Rio Grande silvery minnow as implemented in the NeEstimator version 2.0 software package (Do et al., 2014). Low frequency alleles ($P_{crit} = 0.02$) were excluded from the microsatellite data set singleton alleles were removed for microhaplotypes prior to analysis. Estimates of N_{eD} are an approximation of the effective number of parents that produced the

year class from which the sample was taken (Waples, 2005). For microhaplotypes 95% CIs for N_{eD} were calculated using a jackknife approach recommended for data sets with large numbers of loci (Jones et al., 2016) because parametric confidence intervals are too narrow when locus pairs are not entirely independent (Gilbert & Whitlock, 2015). For consistency, we also used the jackknife method to generate CIs for microsatellites, but these did not differ greatly from parametric CIs. Three estimates of $N_{eD} = \infty$ were obtained across the two data sets (1999, 2000—microsatellites; 2000—microhaplotypes; see Results section). Infinite estimates occur when results can be explained entirely by sampling error, and is usually interpreted as a large value of N_{eD} (Waples & Do, 2010). We used the equation.

$$N_{e(inf)} = N_{e(max)} + SD\ N_e.$$

to adjust estimates for subsequent analysis, where $N_{e(inf)}$ is the value used to replace infinite estimates, $N_{e(max)}$ is the largest N_e estimate obtained, and SD N_e is the standard deviation calculated across all N_e estimates by marker type (Gossieaux et al., 2019).

Variance effective population size (N_{eV}) was calculated using the temporal method (Nei & Tajima, 1981). Confidence intervals for N_{eV} were obtained using the parametric approach (Waples, 1989). We used a $P_{crit} = 0.02$ to exclude low frequency alleles (Waples & Do, 2010) to reduce biased estimates of N_e associated with rare alleles (Hedrick, 1999; Turner et al., 2001). To account for small deviations from the discrete generation model, we corrected consecutive estimates (i.e., 1999–2000, 2008–2009, 2009–2010, 2017–2018) of N_{eV} for overlapping generations as described previously (Osborne et al., 2012; Turner et al., 2006). We used Rosner's Test (Rosner, 1983) to detect outliers in N_{eV} and N_{eD} estimates. Four outlier N_{eD} values (1999, 2000, 2010, 2012) were detected in the microsatellites data. Consequently, a Spearman correlation was used to examine the relationship between N_{eD} estimates obtained with microsatellites and microhaplotypes. Single outlier N_{eV} values were detected in the microsatellite and microhaplotype data set; 2015–2017 and 2002–2004 respectively. Relationships between N_{eV} obtained with microsatellites and microhaplotypes were evaluated using Pearson's correlation as the outliers did not affect this analysis. These analyses were performed in R using the ggpubr package version 0.4.0.999 (Kassambara & Kassambara, 2020).

2.8 | Temporal differentiation

Temporal genetic structure was evaluated using *k*-means clustering to estimate the optimal number of population groups in our data sets and using discriminant analysis of principal components (DAPC). DAPC summarizes genotypes in principal components which are used to construct linear functions that maximize among group variation while minimizing within group variation. Both analyses were performed using the R package adegenet version 1.3–1 (Jombart & Ahmed, 2011). *K*-means clustering was used for de novo group identification, where *k* is the number of groups, using both data sets. A group was defined as a distinct genetic sample taken at a particular time. Bayesian information criteria (BIC) were used to select *k* with the lowest BIC value. Prior to DAPC we replaced missing data within each group using the Breiman's regression random forest algorithm (Breiman, 2001) implemented in R package randomForest version 4.6-14 (Liaw & Wiener, 2002). Values of missing data in the microhaplotype (3% total MD) and microsatellite (2% total MD) data sets were predicted from 500 independently constructed regression trees and 50 bootstrap iterations with default bootstrap sample size. This was preferred over the default "mean method" (i.e., missing genotypes are replaced by the average estimated across the data set) implemented in adegenet to ensure that we did not artificially increase similarity of allele frequencies across years. For each marker type, a first DAPC was performed using years as groups, without scaling allele frequencies, retaining all PCA and DA axes, and keeping other options as default. The *a-score* method was used to select the optimal number of principal components retained for the final DAPC. This analysis was performed using the maximum number of PCs found with the first DAPC, all DAs and the other options were set as default. The final DAPC was performed using the optimal number of PCs, two DAs and keeping the other default options. Levels of diversity (number of alleles and heterozygosity) differ between microsatellites and microhaplotypes (dominated by biallelic SNPs), hence we calculated pairwise values of G''_{ST} (Meirmans & Hedrick, 2011) and 95% CIs between temporal samples using diveRsity for both data sets. Confidence intervals were calculated using 999 bootstrap replicates. We used a Mantel test implemented in R (mantel.rtest) with 9,999 replicates to compare the values of G''_{ST} obtained for microsatellite and microhaplotypes. All analyses were conducted in R studio version 1.3.1093-1 (RStudio Team, 2019) using R version 4.0.3 (R Core Team, 2020).

2.9 | Evaluation of inbreeding metrics for genetic monitoring

In addition to "standard" genetic diversity metrics (Osborne et al., 2012), we added metrics of inbreeding to the genetic monitoring time-series. We calculated standardized multilocus heterozygosity (sMLH) for individuals in each temporal sample based on microsatellite and microhaplotype loci using the R package inbreedR (Stoffel et al., 2016). Measures of inbreeding, including internal relatedness (IR) and mean identity by descent (IBD) inbreeding coefficient ($\overline{F}$), were calculated using the programs GENHET (Coulon, 2010) and EMIBD9 version 1.0 (Wang, 2021), respectively. We used Pearson correlations and biplots to visualize relationships of $\overline{F}$ and sMLH/IR for both data sets.

We measured identity disequilibrium using the $\hat{g}_2$ statistic for each temporal sample (David et al., 2007; Szulkin et al., 2010). To test whether $\hat{g}_2$ was significantly different from zero, genetic data were permutated 1000 times to generate a *p*-value for the null hypothesis of no variance in inbreeding (i.e., $\hat{g}_2 = 0$; David et al., 2007; Stoffel et al., 2016). Bootstrap replicates ($n = 1000$) were used to generate

95% CIs. We used the nonparametric WAVK test (Wang et al., 2008) (with moving window = 3) using the R package funtimes version 8.2 (Lyubchich et al., 2022) to examine if there were any significant trends (monotonic or nonmonotonic) for values of $\overline{F}_{pop}$, $\hat{g}_2$ or F_{IS} over the time series. Values were considered significant when $p < .05$. In cases where a significant trend was detected, we used a Mann-Kendall test (MK; Mann, 1945) to determine if the trend was monotonic (reported as Kendall's τ) using the R package trend (Pohlert, 2020). The magnitude of the change was calculated using Sen's slope (Sen, 1968) at the 5% significance level. The standard normal homogeneity test (SNHT) implemented in trend was used with one million Monte-Carlo replicates to identify transitions (i.e., change-points) when a significant trend was detected (microhaplotype-based $\overline{F}$, $\hat{g}_2$).

3 | RESULTS

3.1 | Variant calling and quality filtering

After sequencing the nextRAD libraries and demultiplexing the raw sequences, an average 3.4 million (M) reads per individual (minimum = 1.1 M; maximum = 5.5 M) were obtained. After alignment to a draft reference genome, an average of 1.27 M reads per individual were retained for further SNP search (minimum = 0.9 M; maximum = 5.3 M). The total number of reads, variants, and individuals retained after each step of the bioinformatics pipeline are shown in Table S2.

3.2 | Quality of samples based on preservation method and year of collection

The median number of mapped reads did not differ significantly between DNA isolated from frozen tissue and purified DNA from archived phenol-chloroform-extracted isolates (Figure S1). Median number of reads was higher for DNA from frozen tissue samples compared to ethanol-preserved material. There were also differences among temporal collections, but the number of mapped reads was relatively high in all cases (3.1–3.4 M reads per individual for all preservation methods).

3.3 | Summary of genetic monitoring data for Rio Grande silvery minnow

The final data set consisted of 3151 loci comprising 5549 SNPs from 366 individuals. Loci that were multiallelic (2–12 alleles per locus) comprised 42.5% of loci. The remainder (57.5%) were single biallelic SNPs. Although we collectively refer to this data set as microhaplotypes, we acknowledge that most loci characterize variation at single sites. Across all years, a total of 8458 microhaplotype alleles were observed compared to microsatellites 240 alleles. Across both data sets (microsatellite and microhaplotypes) we did not observe correlations between the percentage of missing data and diversity metrics (Table S3) with the exception of microhaplotype-based allelic richness ($r_{[df = 11]} = -0.71$, $p = .011$). Likewise, % MD was not correlated with either $\hat{g}_2$ or $\overline{F}_{pop}$ for either data set. Out of 37,932 total HWE tests (3161 loci across 12 years) based on microhaplotypes, 9.1% departed from HWE. No loci departed from HWE consistently across the time-series thus all loci were retained. Additionally, 10 loci were consistently found in LD and discarded, retaining 3151 loci. Of 108 total HWE tests (9 loci across 12 years) based on microsatellite data, departures from HWE were detected in 37% of the tests. Across years, LD was detected between three pairs of microsatellite loci (*Lco6* and *Lco7*; *Lco1* and *Ca6*; *Lco3* and *Ca8*). We retained all loci as we have previously shown that this strategy does not affect downstream analyses (Turner et al., 2006). Microsatellite-based H_O was lower in 1999–2002 and 2009–2010 compared to other years (Figure 2, Table S4). However, overlapping CIs for all microsatellite estimates of H_O and uH_S indicated no difference across time.

Two N_{eD} estimates based on microsatellites (2004 and 2015) and microhaplotypes (2006 and 2015) were smaller than other temporal samples (Figure 3). Conversely, infinite N_{eD} estimates were observed in 1999 for both data sets, and probably resulted from small sample size rather than a true large effective population size. Otherwise, for both data sets, temporal estimates of variance effective population size, N_{eV}, were uniformly about one order of magnitude smaller than estimates of N_{eD} and ranged from 33 (1999–2000) to 604 (2015–2017) for microsatellites and from 122 (2008–2009) to 576 (2002–2004) for microhaplotypes (Table S4).

DAPC based on *k*-means clustering of microhaplotype and microsatellites data indicated the best solution as $k = 1$ (Figure 4). In the DAPC plot based on microsatellites, the 2015, 2017 and 2018 ellipses were shifted to the right on the first discriminant axis indicating a shift in allele frequencies. Microhaplotype-based DAPC exhibits the same qualitative pattern. Values of pairwise G''_{ST} ranged from 0.003 to 0.095 for microsatellites and from 0.002–0.008 for microhaplotypes (Figure S2).

3.4 | Comparisons between microsatellites and microhaplotypes

Gene diversity and H_O obtained from microsatellites were not significantly correlated with those obtained from microhaplotypes (Table 3). Allelic richness was negatively correlated between data sets ($r_{[df = 11]} = -0.70$, $p = .012$); however, the actual difference in microhaplotype-based values of A_R between temporal samples was negligible. Confidence intervals were wider for microsatellites compared with microhaplotypes for all diversity metrics (Figure 2). Estimates of N_{eD} were similar in magnitude between markers and had overlapping confidence intervals across the time series (Table S4, Figure 3). Estimates of N_{eD} from microhaplotypes were significantly correlated with estimates based on microsatellites ($r_{s[df = 11]} = 0.676$, $p = .016$). Microhaplotype-based estimates of N_{eV} were not strongly associated with estimates derived from

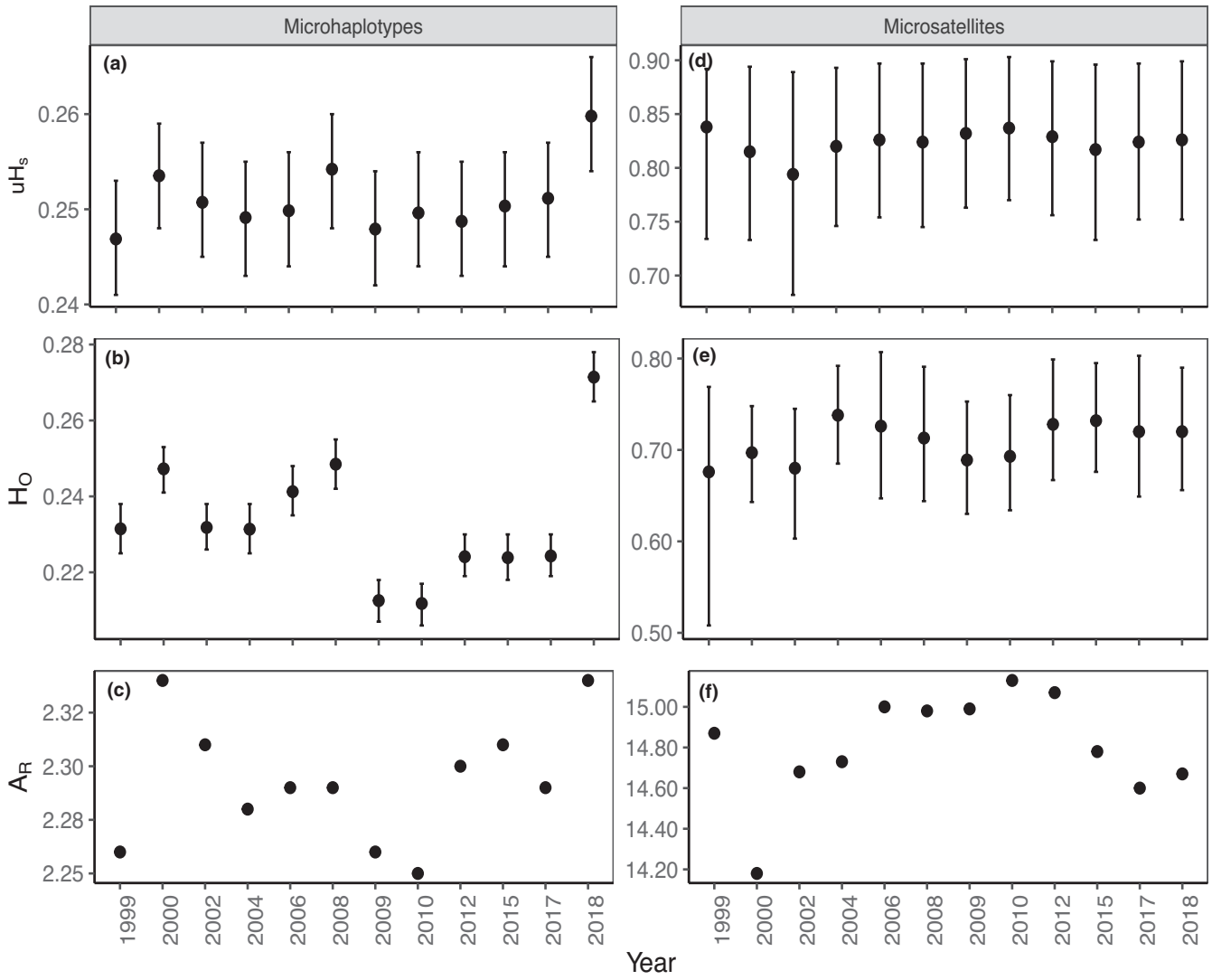

FIGURE 2 Genetic diversity estimates across temporal collections: (a) unbiased heterozygosity (uH_S), (b) observed heterozygosity (H_O) and (c) allelic richness (A_R) based on microhaplotype and microsatellite (d–f) data sets. Note that the y-axis scales are different. For uH_S and H_O the 95% confidence intervals are shown

microsatellites ($r_{[df = 9]} = 0.136$, $p = .689$). Mantel correlations between pairwise values of G''_{ST} obtained using these two data sets were significantly positively associated. Microhaplotype-based estimates of G''_{ST} were small between temporal samples and not different from zero (Figure S2) while microsatellite-based values were significantly different from zero except for comparisons between the most recent temporal collections (2015–2017, 2015–2018).

3.5 | Evaluation of inbreeding metrics for genetic monitoring

When compared with microhaplotypes, sMLH and IR based on microsatellites had a wider range of values within years, but mean values varied little across the time series (Figure 5). Microhaplotype-based values of IR had a narrower range such that an increase in IR could be detected for the period 2009–2017 compared to other years (1999–2016, 2018). This same pattern was not evident from the microhaplotype-based sMLH values. Values of $\overline{F}_{pop}$ calculated from microsatellites varied from 0.13 (2015) to 0.27 (2002) while $\overline{F}_{pop}$ values based on microhaplotypes were smaller ranging from 0.02 (2017) to 0.14 (2018). At the individual level, there was a strong correlation between microsatellite-based sMLH ($r_{[df = 11]} = -0.95$, $p < .00001$) and IBD $\overline{F}$ for microsatellites. This result was mirrored for microhaplotype-based sMLH ($r_{[df = 11]} = -0.76$, $p < .001$; Figure S3). IR was also strongly correlated and IBD $\overline{F}$ regardless of marker type. For both sMLH and IR, the correlation with $\overline{F}$ was stronger for microsatellites compared to microhaplotypes.

No trend was identified by microsatellite-based estimates of $\overline{F}$, $\hat{g}_2$ or F_{IS} or for microhaplotyped-based F_{IS} across the time series (Table S5, Figure 6, Figure S4). Monotonic trends were detected for microhaplotype-based estimates of $\overline{F}_{pop}$ ($\tau = 0.485$; $p = .017$; slope = 0.006, $p = .034$; Figure 6) and $\hat{g}_2$ ($\tau = 0.697$; $p = .001$; slope = 0.001, $p = .002$) which increased across the time series. Microhaplotype-based estimates of F_{IS} and $\overline{F}_{pop}$ had narrower CIs compared to those derived from microsatellites while some of the

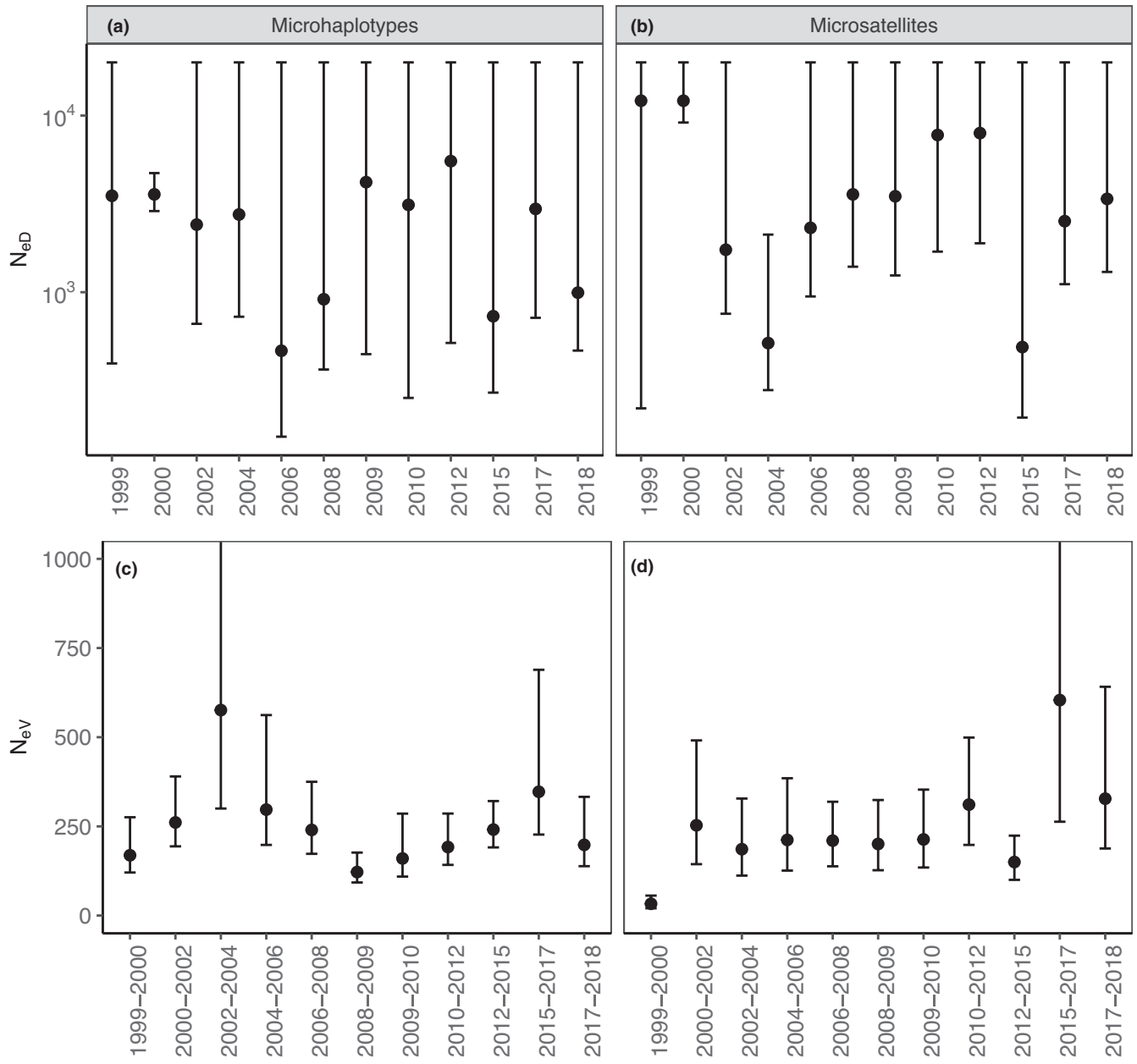

FIGURE 3 Genetic effective population size results based on linkage disequilibrium (N_{eD}) calculated from (a) microhaplotypes and (b) microsatellites and associated 95% confidence intervals. Y-axis is a log scale. Genetic effective population size results based on the variance of allele frequencies (N_{eV}) calculated from microhaplotypes (c) and microsatellites (d) using the method of Nei and Tajima (1981) and associated 95% confidence intervals

CIs for $\hat{g}_2$ were wider for microhaplotype-based estimates but these did not overlap with zero.

4 | DISCUSSION

4.1 | Summary of genetic monitoring data for Rio Grande silvery minnow - insights from microhaplotypes

Two decades of microsatellite-based genetic monitoring in Rio Grande silvery minnow has provided information critical to ongoing adaptive management (Table 4). Conclusions from microhaplotype data largely agree with interpretations based on microsatellites but inclusion of additional metrics provide additional insight into the complex dynamics in this population. Microhaplotype-based estimates of diversity reinforces that genetic variation has been maintained despite periodic population collapse. This resilience is attributable to ongoing population augmentation and integrated management of wild and captive populations (Osborne et al., 2012, 2020). More precise population and individual diversity estimates (uH_S, H_O, IR) based on microhaplotypes revealed patterns of genetic change over time not detected by microsatellites; highlighting one of the benefits of transitioning to microhaplotype-based genomic monitoring. Additionally, microhaplotypes were more sensitive to shifts in temporal genetic diversity where DAPC clearly indicated a

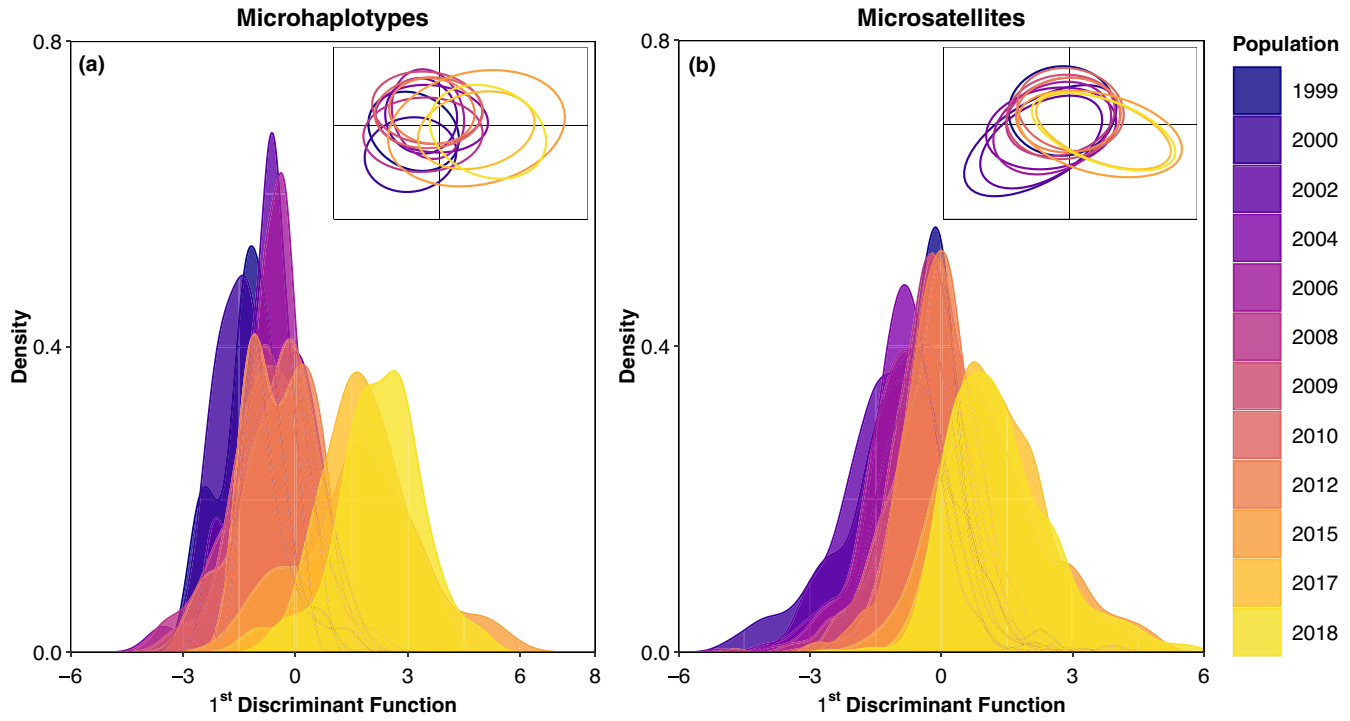

FIGURE 4 Results of discriminant analysis of principal components (DAPC) based on (a) microhaplotypes and (b) microsatellite data. In each panel the curves represent the density of individuals across the first discriminant function (DF) axis. The first DF axis explained 35% of the variance for microhaplotypes and 37% of the variance for microsatellites. The inset in each panel shows the ellipses representing the 95% confidence level for a multivariate normal distribution, plotted on the first and second DF axes. Colours represent temporal samples

TABLE 3 Pearson's correlation coefficients for genetic metrics (unbiased gene diversity [*u*Hs], observed heterozygosity [H_O], allelic richness [A_R], average inbreeding coefficient [F_{IS}], variance effective population size (N_{eV}), and mantel correlation for G''_{ST} and Spearman's correlation for linkage disequilibrium effective population size [N_{eD}]) and calculated between microhaplotypes and microsatellites and associated *p*-values (significant values are denoted by an asterisk)

Metric	Correlation	*p*-value
uH_S	−0.220	.490
H_O	0.190	.550
A_R	−0.700	.012*
F_{IS}	0.230	.480
N_{eV}	0.136	.689
G''_{ST}	0.153	.023*
N_{eD}	0.676	.016*

distinct allele frequency shift. Larger shifts corresponded to periods of extremely low wild abundance when heavy population augmentation was employed to replenish the wild spawning stock resulting in genetic drift. A persistent allele frequency shift after 2014 marks the replacement of the wild population with stocks derived from relatively few captive breeders (i.e., slightly different allele frequencies compared to the pre-bottleneck population).

Microhaplotype-based estimates of contemporary genetic effective size were also consistent with microsatellites in showing that N_{eV} is small (<250) for most pairwise comparisons, and values of N_{eV} are consistently smaller than N_{eD}. Estimates of N_{eV} generally had tight confidence intervals regardless of data types, confirming that alternative sampling strategies that use (1) more individuals but fewer loci (microsatellites), or (2) fewer individuals but more loci (microhaplotypes) have similar power to estimate this metric (e.g., Waples, 1989). Consistency of results obtained from microhaplotypes with previous microsatellite data is important as contemporary N_e is a critical determinant of diversity loss from the population. The smallest values of N_{eD} (both data types) were seen in samples collected immediately following population bottlenecks (2004, 2006, 2015). These findings are consistent with Antao et al. (2010) who found that N_{eD} reliably detected less severe population declines a few generations after the event.

The underlying causes for differences between N_{eV} and N_{eD} have been explored previously. Briefly, Carson et al. (2020) used simulations to show that N_{eD} and N_{eV} respond differently to augmentation and dispersal/ fragmentation. Specifically, N_{eD} measured in the wild population reflects the global effective size of the total population (wild + hatchery) and hence at higher augmentation rates N_{eD} should be larger. In contrast, augmentation has the opposite effect on N_{eV} because augmentation acts as an additional source of "genetic drift" such that N_{eV} is reduced with heavier augmentation. In reality, N_{eV} and N_{eD} estimated for the Rio Grande silvery minnow population do not always respond as predicted because simulations cannot capture all complex interactions between demography of the wild population that experiences large swings in population size from year to year, with simultaneous management actions.

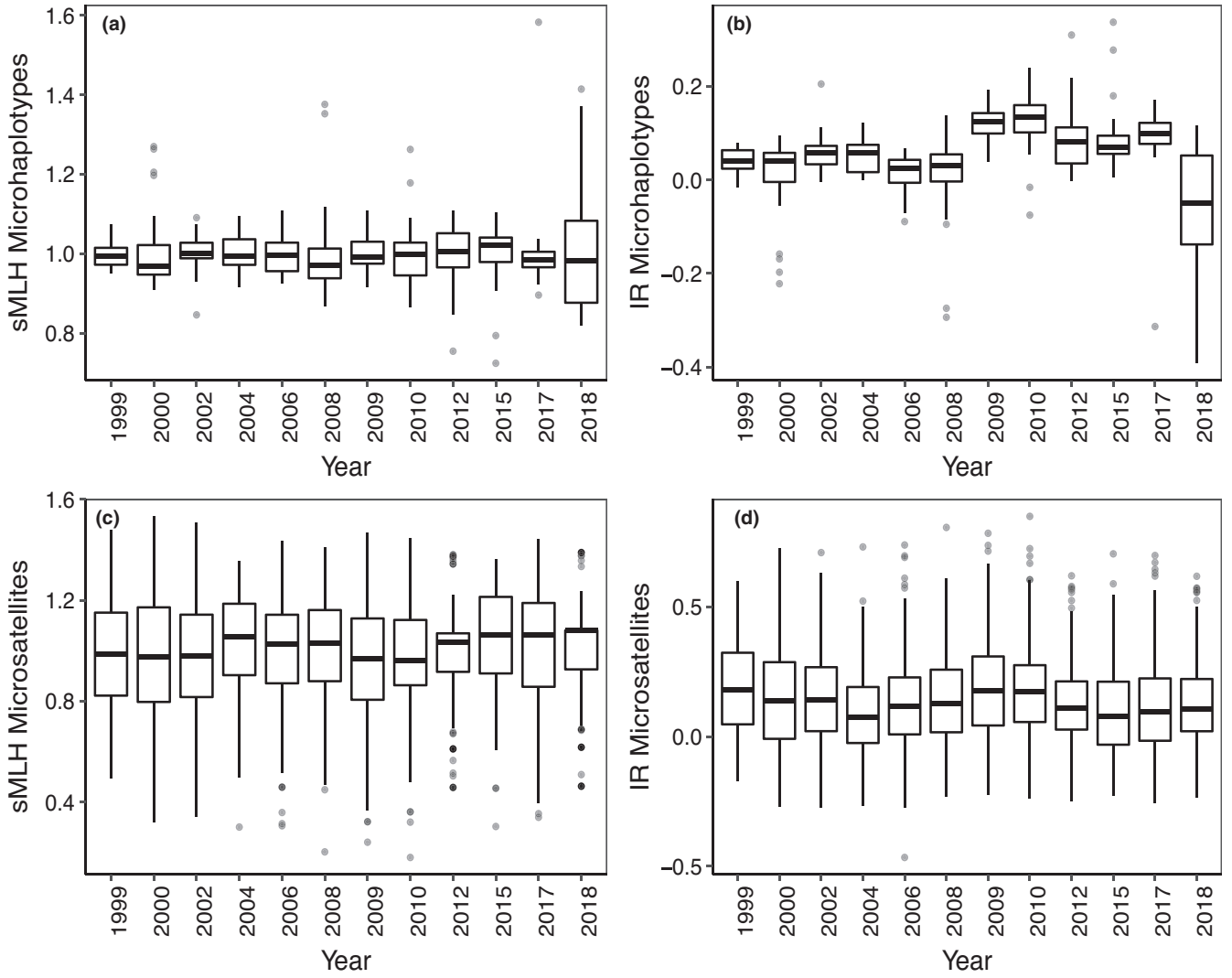

FIGURE 5 (a) Mean standardized multilocus heterozygosity (sMLH) and (b) mean internal relatedness (IR) for temporal samples based on microhaplotypes, and (c, d) microsatellites

Genomic signatures of population bottlenecks and augmentation were also revealed by considering measures of inbreeding not traditionally used in genetic monitoring programmes. Trends in $\hat{g}_2$ and $\overline{F}$ calculated from microhaplotypes suggested that incorporating these metrics into genetic monitoring programmes would be a valuable addition and could enable study of relationships of GWH to fitness in a managed population. Further investigation is necessary to fully understand how these metrics respond to complex demographic scenarios. Microsatellites appeared to be less sensitive to these temporal trends probably because of the small number of loci compared to microhaplotypes.

4.2 | Comparisons between microsatellites and microhaplotypes

Comparisons of microsatellites and microhaplotypes allowed us to evaluate the relative consistency, precision, and sensitivity to missing data between marker types (Table 5). Of all the metrics we evaluated, we found that only microhaplotype-based estimates of A_R were sensitive to the low levels of missing data in our study. Even with relatively small sample sizes, microhaplotypes yielded more precise estimates of diversity (uH_S, H_O IR) and N_{eV} compared to microsatellites, allowing temporal changes to be detected in the time-series. On the other hand, microhaplotye-based A_R was not an informative metric. Like other studies (e.g., Fischer et al., 2017; Lemopoulos et al., 2019; Zimmerman et al., 2020) and important for ongoing monitoring efforts in Rio Grande silvery minnow, we found that measures of divergence (G''_{ST}) were positively correlated between markers and this was also true of N_{eD}. Hence, when these metrics (G''_{ST} and N_{eD}) are measured with only SNP-based markers in the near future, we can be relatively confident that signals of divergence or changes in effective population size are accurate rather than a consequence of change in marker type. Although CIs were often large for N_{eD} regardless of data type, trends in annual point estimates makes N_{eD} a particularly important metric for adaptive species management when interpreted in the context of population demography.

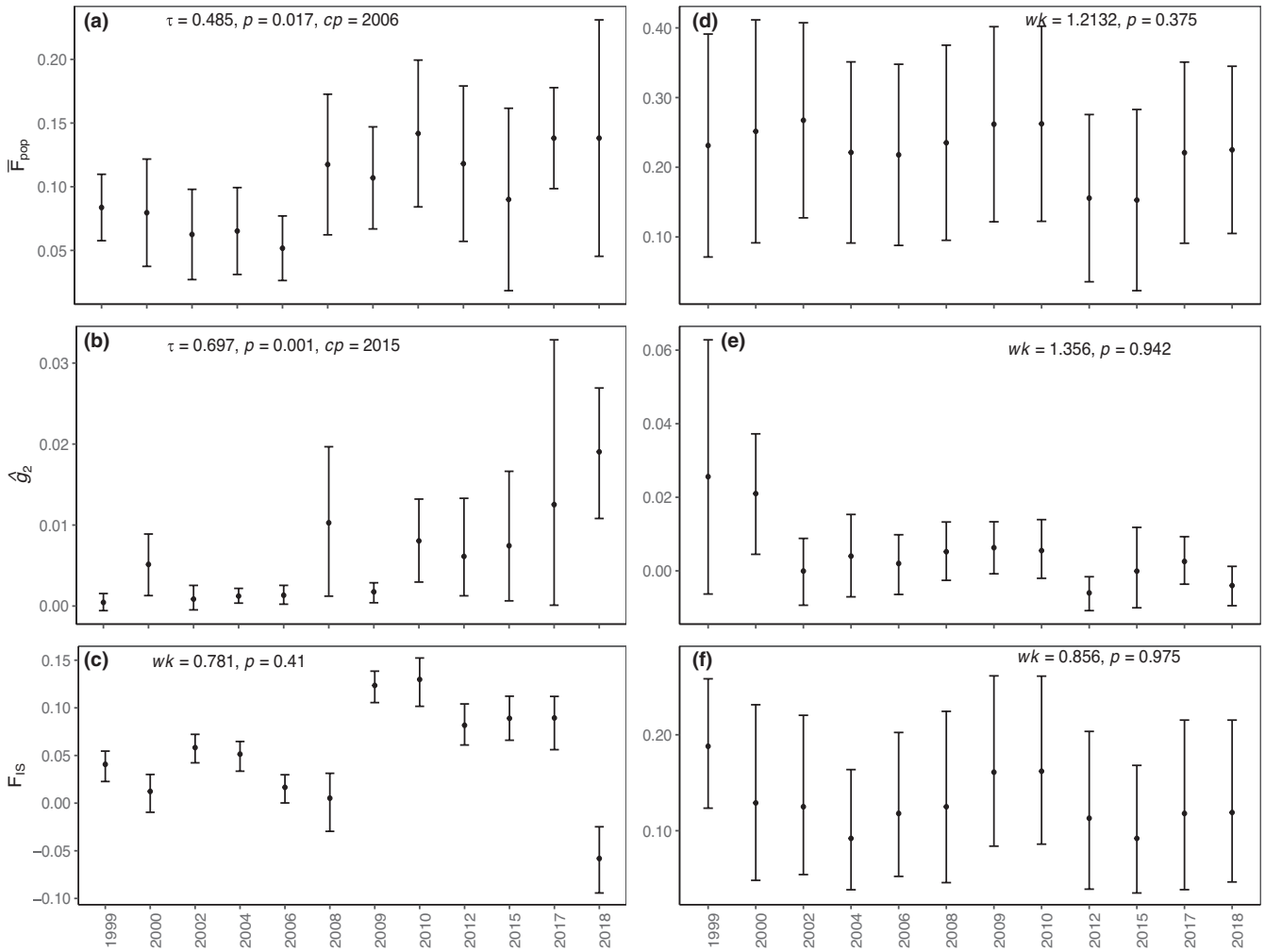

FIGURE 6 (a) Average IBD $\overline{F}_{pop}$ (b) identity disequilibrium ($\hat{g}_2$), and (c) F_{IS} for temporal samples based on microhaplotypes, and (d–f) and microsatellites. Associated 95% confidence intervals are shown for $\hat{g}_2$ and F_{IS}, and standard deviation is given for $\overline{F}_{pop}$. The WAVK test statistics (*wk*) and *p*-values are shown for nonsignificant tests. Mann-Kendall's τ and *p*-values, and change-points (cp) are shown when significant monotonic trends were detected

Weak correlation of diversity metrics between data sets suggests that diversity estimated from a small number of microsatellites may not sufficiently reflect genomic diversity (Guillot & Foll, 2009; Lemopoulos et al., 2019). Other studies failed to find significant correlations between some diversity metrics estimated from microsatellites and SNPs (e.g., DeFaveri et al., 2013; Fischer et al., 2017; Zimmerman et al., 2020). Chakraborty (1981) and DeFaveri et al. (2013) concluded that variation in heterozygosity across the genome would result in lack of correlation of diversity measures when estimates from a small number (<20) of molecular markers; such as in our study. Lack of correlation between markers sets for uH_S and H_O may also be caused by (1) ascertainment bias, (2) typing artefacts (microsatellites), (3) underlying evolutionary processes affecting per locus levels of diversity, and (4) genomic location of the markers (e.g., DeFaveri et al., 2013).

Microsatellites are typically found in noncoding regions of the genome such as introns and intergenic regions and evolve primarily by replication slippage, and thus have high mutation rates (Ellegren, 2004). Loci are typically selected for population genetic studies based on levels of diversity such that more polymorphic loci (higher number of alleles and heterozygosity) are preferred, yielding greater sensitivity to changes in population size and genetic diversity. Reductions in microsatellite allelic diversity were detected in Rio Grande silvery minnow from 1999 to 2000 (before population augmentation began) and in 2012 and 2015 that bracketed order of magnitude declines in the middle Rio Grande population. Substantial declines in allelic diversity were not seen in the rest of the time series (except in 2017), a result that we attribute to repeated population augmentation (Osborne et al., 2012). Despite this reduced sensitivity, our results suggest declines in A_R were not detected with microhaplotypes because loci are dominated by biallelic SNPs. Our results suggest that SNPs obtained from high throughput NGS protocols could be more important to monitor as they represent a broader picture of genomic variation as many more loci as assayed including coding and noncoding regions.

TABLE 4 A comparison of key findings and recommendations based on microsatellite data and microhaplotype data for Rio Grande silvery minnow

Key finding	Micro-satellites	Micro-haplotypes	Underlying biological process	Management recommendations
Genetic diversity metrics stable over a 20-year time series	Yes	Yes[a]	Sufficient diversity remains in wild and hatchery stocks to maintain "neutral" genetic diversity despite large population fluctuations	The comprehensive adaptive management strategy is meeting many targets for "neutral" genetic diversity.[1, 2]
Low A_R in some captive brood stocks	Yes	Not tested[b]	Too few captive spawners to form a representative brood stock	Increase broodstock numbers, spawning, and rearing capacity in multiple facilities.[3]
Inbreeding trends detected?	No	Yes[c]	Microhaplotypes have more power to detect inbreeding but further evaluation is necessary	Increase broodstock numbers, spawning, and rearing capacity in multiple facilities.[3]
Wild-caught drifting eggs (WCE) sufficiently represent whole-population genetic diversity	Yes	Not tested	Spawning is triggered by spring snowmelt flow pulse, eggs drift downstream. Multiple flow peaks initiate multiple spawning events	Temporal sampling interval should span the entire spawning season. Eggs should be collected from all river reaches. WCE prioritized for augmentation and refugial broodstock.[2, 4, 5]
$F_{ST} \approx 0$ across Rio Grande sampling localities	Yes	Not tested	High dispersal and gene flow throughout the current species range. Downstream-biased egg and larval dispersal	Collect broodstock from all river reaches (i.e., the species range) to maximize diversity. It is not necessary to create geographically distinct stocks.[1, 4, 6, 7]
$N_e/N << 0.1$ in wild populations	Yes	Yes	Downstream transport of pelagic eggs past dams introduces high variance in reproductive success (VRS) among spawning aggregates. Other species exhibit $N_e/N \geq 0.1$	Re-engineer dam and diversion structures to allow for upstream fish passage. Restore connectivity to lateral floodplain habitat to enhance egg retention and recruitment.[1, 4, 6, 7]
N_{eV} is not correlated with N in wild populations	Yes	Not tested[d]	Inputs from the hatchery and VRS strongly influence the relationship of N_e and N	N_e is not a proxy for wild abundance. Demographic and genetic monitoring are required to evaluate ecological and evolutionary effects of population fluctuation and hatchery inputs.[1, 7, 8]

Note: Hypothesized biological processes that underlie key findings are listed, as are management recommendations that emerged from key findings. References are provided for microsatellite data. Inferences based on microhaplotypes are described in the text.

[1]Osborne et al. (2012), [2]Osborne et al. (2020), [3]Osborne et al. (2006), [4]Osborne et al. (2005), [5]United States Fish and Wildlife Service (2018a), [6]Alò and Turner (2005), [7]Turner et al. (2006), [8]Carson et al. (2020).

[a]Not all metrics perform equally well across marker classes (see text).

[b]Not explicitly tested, but A_R is not an effective metric for microhaplotype data.

[c]Microhaplotypes are more sensitive to inbreeding effects or have more power to detect them.

[d]Not tested.

Low allelic variability at individual microhaplotype loci is offset by a substantially higher number of loci such that the larger number of total number of alleles assayed yielded more precise estimates of diversity (i.e., smaller confidence intervals) when compared with microsatellites in Rio Grande silvery minnow. For example, microhaplotype-based heterozygosity was higher in 2018 (and IR was lower) compared to previous years reflected by a negative inbreeding coefficient while F_{IS} and IR increased between 2009–2017 compared to values observed from 1999–2008. These changes are indicative of departures from Hardy–Weinberg proportions. An excess of heterozygotes in 2018 and deficit in 2009–2017 is probably a "Wahlund" or sampling effect (Waples, 2015) that occurred when fish from the middle Rio Grande population and different hatchery sources were mixed by augmentation. Different proportions of wild to captive fish may also affect the value of F_{IS} because the magnitude of the Wahlund effect increases with population divergence in allele frequencies and the evenness of mixture proportions (Waples, 2015).

TABLE 5 Summary of differences/similarities of genetic metrics between data sets and broad conclusions

	Genetic metric	Microsatellites	Microhaplotypes	Conclusions
Individual metrics	sMLH/IR/$\overline{F}$	Strong correlation between sMLH and IBD $\overline{F}$	Strong correlation between sMLH and IBD $\overline{F}$	sMLH/IR—reflect IBD $\overline{F}$. Microhaplotypes detect temporal changes in individual diversity
	$\hat{g}_2 / \overline{F}_{pop}$	Wide CIs for sample Most $\hat{g}_2$ estimates not >0	Narrow CIs. $\hat{g}_2 > 0$	Microsatellites lack power to estimate inbreeding/ID via $\hat{g}_2$ in most cases. Temporal changes in inbreeding ($g_2 / \overline{F}_{pop}$) detected across time series by microhaplotypes
Population metrics	(uH_E, H_O, F_{IS}, A_R)	Overlapping CIs No trend apparent for uH_E, H_O, F_{IS}. Reduced A_R in some years corresponding to reduced abundance	Narrow CIs, increased precision Years with increased values of F_{IS}	Temporal patterns differ, but both data sets show genetic diversity maintained. Increased precision of microhaplotype-based estimates allows small differences between temporal samples to be detected (i.e., F_{IS} and H_O)
Temporal divergence	DAPC	Weak temporal divergence	Temporal divergence between old and more recent samples	Temporal shift in allele frequencies detected from microhaplotypes
	G''_{ST}	Range: 0.003–0.095/ Smaller CIs	Range: 0.002–0.008 Overlapping CIs	Strongly correlated. Small degree of divergence between temporal collections. Smaller values for microhaplotype-based estimates
	Mean G''_{ST}	0.03	0.004	
Effective population size	N_{eV}	N_{eV} = 33–604 Overlapping CIs	N_{eV} = 122–576 Narrow CIs, increased precision	N_{eV} is small. Both data sets show an increase in N_{eV} for 2015–2017 and decrease between 2017–2018. Differences between N_{eV} estimates can be identified with microhaplotypes
	N_{eD}	Wide CIs N_{eD} = 489–12,127	Wide CIs N_{eD} = 731–3579	Strongly correlated. Both data sets detect an order of magnitude decline associated with population collapse in 2012–2014

4.3 | Evaluation of inbreeding metrics for genetic monitoring

In Rio Grande silvery minnow, we found that sMLH and IR were strongly associated with $\overline{F}$ and F_{IS} for both data sets. The strength of observed correlations between individual $\overline{F}$ and sMLH and IR in Rio Grande silvery minnow was greater than in other species including zebra finch (range $r^2 = 0.46–0.49$; Forstmeier et al., 2012) but within the range seen in oldfield mice ($r^2 = 0.74$; Hoffman et al., 2014). Strong correlations were also reported between genomic measure of inbreeding based on runs of homozygosity (F_{ROH}) and heterozygosity (MLH) in wolves ($r^2 = 0.91$; Kardos et al., 2018). The genomic measures of inbreeding used here (e.g., MLH, IR, $\hat{g}_2$) characterize variation in inbreeding due to all IBD segments of the genome including those arising from both recent and distant ancestors (Kardos et al., 2018; Keller et al., 2011). These metrics may be more accurate than alternative pedigree-based estimates that make the unrealistic assumption of unrelated ancestors. In cases where there is high variance in $\overline{F}$ (e.g., 2018), genomic measures of individual inbreeding (e.g., IR and sMLH) are expected to be more precise (Kardos et al., 2018, 2014; Miller et al., 2014); consistent with microhaplotype data.

Variance in inbreeding in some years (Figure 6, Figure S4) was also reflected in microhaplotype-based values of $\hat{g}_2$ that were significantly different from zero. In contrast, most microsatellite-based $\hat{g}_2$ values were not informative about underlying identity by descent because in the majority of cases, $\hat{g}_2$ did not differ from zero. Other authors (e.g., Hoffman et al., 2014; McLennan et al., 2019) also found that compared with microsatellites, $\hat{g}_2$ estimated from large numbers of SNP-based markers provided a more accurate measure of inbreeding and GWH because of increased statistical power associated with the number of SNP loci screened. Likewise, Kardos et al. (2014) found that when estimated from few microsatellite loci $\hat{g}_2$, was not significant even in cases when heterozygosity fitness correlations were present.

Identity disequilibrium ($\hat{g}$) can occur when genetic drift/bottlenecks yield a higher incidence of consanguineous matings as a consequence of small population size. Moreover, populations that have experienced multiple bottlenecks may have inflated inbreeding values (Robinson et al., 2013). Miller et al. (2014) found that ID was substantially higher ($\hat{g}_2 = 0.06$) in a population of bighorn sheep that had experienced a population bottleneck and was subsequently "rescued" by introduction of individuals from a neighbouring population, when compared to a native population ($\hat{g}_2 = 0.004$). Values of $\hat{g}_2$ observed in Rio Grande silvery minnow at several time-points ($\hat{g}_2 = 0.01–0.019$ in 2008, 2017–2018) are considered high for a natural population (Hoffman et al., 2014). For example, most microhaplotype-based values of $\hat{g}_2$ in Rio Grande silvery minnow were larger than in a small red deer population (*Cervus elaphus*; $\hat{g}_2 = 0.001$; Huisman et al., 2016) and in a large population in storm petrel (*Oceanodroma leucorhoa*; $\hat{g}_2 = 0.001$; Sin et al., 2021). Like Rio Grande silvery minnow, the population of deer has experienced bottlenecks and admixture between different populations (Huisman et al., 2016). Sin et al. (2021) noted that in storm petrel, mating system and inbreeding between close relatives could not account for variance in inbreeding, and hence, suggested that observed variance in inbreeding was explained by past population bottlenecks along with more recent declines in N_e and low levels of admixture between Atlantic and Pacific populations of petrels. Footprints of bottlenecks persist even after the population has recovered (Bierne et al., 2000) and can still cause inbreeding depression (Sin et al., 2021).

Values of microhaplotype-based inbreeding metrics were notably higher for the majority of recent time points from 2008 to 2018 compared to earlier periods (1999–2006). Early augmentation efforts (2002–2007) of the wild population of Rio Grande silvery minnow were comprised largely of stocks reared from wild-caught eggs (WCE) rather than offspring of captive spawning. Stocks reared from WCE typically have allele frequencies nearly identical to the wild population (Osborne et al., 2012). After that time, released fish were increasingly derived from captive spawning and hence derived from fewer parents than wild-produced stocks. Some increases in microhaplotype-based values of $\overline{F}_{pop}$ and $\hat{g}_2$ follow periods of heavy population augmentation (Figure 1). For example, the estimated breeding population in the spring of 2007 was comprised of roughly equal numbers of wild and augmented fish while from 2013 to 2015 the number of augmented fish far exceeded the number of "wild-born" individuals as efforts were made to rebuild the population following its collapse during the drought from 2012 to 2014 (Yackulic et al., 2022). Drought years represent periods when genetic drift is expected to be high because (1) the bottleneck reduces the number of breeders, (2) captive spawning involves only a subset of the population, and (3) only a subset of hatchery fish persist after release. Rio Grande silvery minnow exhibits type III survivorship such that females are highly fecund (Caldwell et al., 2019) but in the wild there is very high mortality of early life stages such that a small proportion of the offspring survive to recruit to the riverine adult population (Horwitz et al., 2018). In contrast, use of captive spawning reduces variance in reproductive success among captive spawners and their offspring are eventually released to the river. In the following year, there may be breeding between slightly related individuals (reflected by larger values of *F*) as well as breeding between relatively unrelated individuals (e.g., wild with augmented fish, and smaller values of *F*); resulting in greater variance in population *F* and reflected by significant values of $\hat{g}_2$ (e.g., 2018). Admixture between populations with different allele frequencies causes gametic associations (i.e., LD) between loci as a function of the difference between the parental populations and the admixture rate (Chakraborty & Weiss, 1988) and the effects of admixture can be variable and can either increase or decrease GWH depending on the magnitude of admixture and the genetic background of the population (Vendrami et al., 2020). Importantly, in both red deer and storm petrel where variance in inbreeding was less than seen recently in Rio Grande silvery minnow, general effects HFC were observed implying inbreeding depression in both a small (Huisman et al., 2016) and a large population (Sin et al., 2021). Hence, inclusion of inbreeding metrics in genetic monitoring of both wild and captive populations of Rio Grande silvery

minnow can provide valuable information for adaptive management of the species (e.g., altered augmentation strategies).

4.4 | Recommendations for genetic monitoring of Rio Grande silvery minnow

For ongoing genetic monitoring in Rio Grande silvery minnow, a subset of the loci used in this study will be incorporated into a genotyping-in-thousands by sequencing panel (GT-seq; Campbell et al., 2015). This is a method of targeted SNP genotyping that uses multiplexed PCR amplicon sequencing and allows consistent genotyping of hundreds of target SNPs across hundreds to thousands of individuals. For genetic monitoring programmes, GT-seq is time and cost-effective once multiplexed PCRs are optimized. (Campbell et al., 2015). Additionally, GT-seq panels should allow consistent genotyping across laboratories which can be troublesome with microsatellites without considerable validation. Preliminary results show that 300 loci are sufficient to represent patterns of population and individual diversity contained in the complete data set presented in this study (data not shown). Our results demonstrate that it is now possible for conservation programmes to incorporate genomic methods into routine monitoring. Development of genomic tools for this species and others will allow (1) less expensive monitoring, (2) more rapid evaluation of captive stocks prior to release to the wild, (3) retrospective analysis of archived wild and captive material and (4) will facilitate further evaluation of inbreeding metrics and selection.

More broadly, results presented herein highlight the importance of archiving both tissue and DNA samples collected during long-term monitoring so they can be utilized as new genomic technologies are developed. Despite differences in ages of genetic samples and differences in how samples were stored, sequencing depth was sufficient to estimate parameters of interest with generally greater precision than microsatellite data. Archiving biological material (preferably tissue) is important not only for imperilled species with ongoing genetic monitoring programmes, like Rio Grande silvery minnow, but also for species of conservation concern without established conservation programmes; guaranteeing the availability of genetic material in the future. In the case of Rio Grande silvery minnow and many other imperilled species, sampling is often nondestructive so there may not be tissue samples remaining after DNA isolation and in these cases archiving DNA samples along with associated metadata is imperative. Our results are encouraging as they suggest that researchers have some flexibility in sample choice including DNA isolates when transitioning from one marker set to another.

AUTHOR CONTRIBUTIONS

Megan J. Osborne was responsible for project conception, design and coordination, laboratory work, data analysis, manuscript writing and revision, and obtaining funding. Guilherme Caeiro-Dias was responsible for bioinformatics, data analysis, and writing the manuscript. Thomes F. Turner was responsible for project conception, sample curation, manuscript writing and revision and obtaining funding.

ACKNOWLEDGEMENTS

We sincerely thank Alexander Cameron, David Camak, Samuel McKitrick for assistance in the field, laboratory, and with bioinformatics. We thank Emily DeArmon and Alexandra Snyder in the UNM Museum of Southwestern Biology Division of Fishes for expert curatorial services. Thomas Archdeacon (U.S. Fish and Wildlife Service), Charles Yackulic (U.S. Geological Service) provided data, discussions, and insights that greatly improved the manuscript. Comments from four anonymous reviewers improved the manuscript. High performance computing was conducted at the UNM Center for Advanced Research Computing that is supported, in part, by the National Science Foundation. We also thank Eric Gonzales and Jennifer Bachus (U.S. Bureau of Reclamation). This study was funded by the U.S. Bureau of Reclamation (R18AP00130). Samples were collected under permits from the New Mexico Department of Game and Fish (3015), U.S. Fish and Wildlife Service (TE38055-0), and a protocol approved by the UNM Institutional Animal Care and Use Committee (no. 21-201194-MC).

CONFLICT OF INTEREST

The authors declare no conflicts of interest.

DATA AVAILABILITY STATEMENT

Individual genotype data from microsatellites and microhaplotypes are available on Dryad: https://doi.org/10.5061/dryad.bk3j9kdfj. Raw sequence reads from nextRAD-seq (379 individuals), are deposited in the NCBI Sequence Read Archive (SRA), with the BioProject accession number PRJNA887477.

BENEFIT-SHARING STATEMENT

Results of our research have been shared with the broader scientific and management community (see above), and our study addresses a priority concern, specifically the conservation of Rio Grande silvery minnow. Benefits from this research accumulate from the sharing of our data and results on public databases as described above. Results have also been shared with management agencies charged with conservation of the species.

ORCID

Megan J. Osborne https://orcid.org/0000-0002-0978-2905
Guilherme Caeiro-Dias https://orcid.org/0000-0002-5771-6208

REFERENCES

Alò, D., & Turner, T. F. (2005). Effects of habitat fragmentation on effective population size in the endangered Rio Grande silvery minnow. *Conservation Biology*, *19*(4), 1138–1148. https://doi.org/10.1111/j.1523-1739.2005.00081.x

Amos, W., Worthington Wilmer, J., Fullard, K., Burg, T. M., Croxall, J. P., Bloch, C. D., & Coulson, T. (2001). The influence of parental relatedness on reproductive success. *Proceedings of the Royal Society of London. Series B: Biological Sciences*, *268*(1480), 2021–2027.

Antao, T., Pérez-Figueroa, A., & Luikart, G. (2010). Early detection of population declines: High power of genetic monitoring using effective population size estimators. *Evolutionary Applications*, *4*(1), 144–154. https://doi.org/10.1111/j.1752-4571.2010.00150.x

Archdeacon, T. P. (2016). Reduction in spring flow threatens Rio Grande silvery minnow: Trends in abundance during river intermittency. *Transactions of the American Fisheries Society*, *145*(4), 754–765. https://doi.org/10.1080/00028487.2016.1159611

Archdeacon, T. P., Diver-Franssen, T. A., Bertrand, N. G., & Grant, J. D. (2020). Drought results in recruitment failure of Rio Grande silvery minnow (*Hybognathus amarus*), an imperiled, pelagic broadcast-spawning minnow. *Environmental Biology of Fishes*, *103*(9), 1033–1044. https://doi.org/10.1007/s10641-020-01003-5

Archdeacon, T. P., & Reale, J. K. (2020). No quarter: Lack of refuge during flow intermittency results in catastrophic mortality of an imperiled minnow. *Freshwater Biology*, *65*(12), 2108–2123. https://doi.org/10.1111/fwb.13607

Baetscher, D. S., Clemento, A. J., Ng, T. C., Anderson, E. C., & Garza, J. C. (2018). Microhaplotypes provide increased power from short-read DNA sequences for relationship inference. *Molecular Ecology Resources*, *18*(2), 296–305. https://doi.org/10.1111/1755-0998.12737

Balloux, F., Amos, W., & Coulson, T. (2004). Does heterozygosity estimate inbreeding in real populations? *Molecular Ecology*, *13*(10), 3021–3031. https://doi.org/10.1111/j.1365-294x.2004.02318.x

Beatty, G. E., Reid, N., & Provan, J. (2014). Retrospective genetic monitoring of the threatened yellow marsh saxifrage (*S. axifraga hirculus*) reveals genetic erosion but provides valuable insights for conservation strategies. *Diversity and Distributions*, *20*(5), 529–537.

Bennett, J. H., & Binet, F. E. (1956). Association between Mendelian factors with mixed selfing and random mating. *Heredity*, *10*(1), 51–55. https://doi.org/10.1038/hdy.1956.3

Bestgen, K. R., & Platania, S. P. (1991). Status and conservation of the Rio Grande silvery minnow, Hybognathus amarus. *The Southwestern Naturalist*, *36*(2), 225–232. https://doi.org/10.2307/3671925

Bierne, N., Tsitrone, A., & David, P. (2000). An inbreeding model of associative overdominance during a population bottleneck. *Genetics*, *155*(4), 1981–1990. https://doi.org/10.1093/genetics/155.4.1981

Bootsma, M. L., Miller, L., Sass, G. G., Euclide, P. T., & Larson, W. A. (2021). The ghosts of propagation past: Haplotype information clarifies the relative influence of stocking history and phylogeographic processes on contemporary population structure of walleye (*Sander vitreus*). *Evolutionary Applications*, *14*(4), 1124–1144. https://doi.org/10.1111/eva.13186

Breiman, L. (2001). Random forests. *Machine Learning*, *45*(1), 5–32.

Caldwell, C. A., Falco, H., Knight, W., Ulibarri, M., & Gould, W. R. (2019). Reproductive potential of captive Rio Grande silvery minnow. *North American Journal of Aquaculture*, *81*(1), 47–54.

Campbell, N. R., Harmon, S. A., & Narum, S. R. (2015). Genotyping-in-thousands by sequencing (GT-seq): A cost-effective SNP genotyping method based on custom amplicon sequencing. *Molecular Ecology Resources*, *15*(4), 855–867.

Carson, E. W., Osborne, M. J., & Turner, T. F. (2020). Relationship of effective size to hatchery supplementation and habitat connectivity in a simulated population of Rio Grande silvery minnow. *North American Journal of Fisheries Management*, *40*(4), 922–938. https://doi.org/10.1002/nafm.10453

Chakraborty, R. (1981). The distribution of the number of heterozygous loci in an individual in natural populations. *Genetics*, *98*(2), 461–466. https://doi.org/10.1093/genetics/98.2.461

Chakraborty, R., & Weiss, K. M. (1988). Admixture as a tool for finding linked genes and detecting that difference from allelic association between loci. *Proceedings of the National Academy of Sciences*, *85*(23), 9119–9123. https://doi.org/10.1073/pnas.85.23.9119

Coltman, D. W., Pilkington, J. G., Smith, J. A., & Pemberton, J. M. (1999). Parasite-mediated selection against inbred Soay sheep in a free-living, Island population. *Evolution*, *53*(4), 1259–1267. https://doi.org/10.2307/2640828

Coulon, A. (2010). GENHET: An easy-to-use R function to estimate individual heterozygosity. *Molecular Ecology Resources*, *10*(1), 167–169. https://doi.org/10.1111/j.1755-0998.2009.02731.x

David, P., Pujol, B., Viard, F., Castella, V., & Goudet, J. (2007). Reliable selfing rate estimates from imperfect population genetic data. *Molecular Ecology*, *16*(12), 2474–2487. https://doi.org/10.1111/j.1365-294x.2007.03330.x

DeFaveri, J., Viitaniemi, H., Leder, E., & Merilä, J. (2013). Characterizing genic and nongenic molecular markers: Comparison of microsatellites and SNPs. *Molecular Ecology Resources*, *13*(3), 377–392. https://doi.org/10.1111/1755-0998.12071

DeWoody, Y. D., & DeWoody, J. A. (2005). On the estimation of genome-wide heterozygosity using molecular markers. *Journal of Heredity*, *96*(2), 85–88. https://doi.org/10.1093/jhered/esi017

Do, C., Waples, R. S., Peel, D., Macbeth, G. M., Tillett, B. J., & Ovenden, J. R. (2014). NeEstimator: Re-implementation of software for the estimation of contemporary effective population size from genetic data. *Molecular Ecology Resources*, *14*(1), 209–214. https://doi.org/10.1111/1755-0998.12157

Dowling, T. E., Turner, T. F., Carson, E. W., Saltzgiver, M. J., Adams, D., Kesner, B., & Marsh, P. C. (2014). Time-series analysis reveals genetic responses to intensive management of razorback sucker (*Xyrauchen texanus*). *Evolutionary Applications*, *7*(3), 339–354. https://doi.org/10.1111/eva.12125

Dudley, R., Platania, S., & White, G. (2021). *Rio Grande silvery minnow population monitoring during 2020*. U.S. Bureau of Reclamation. https://doi.org/10.13140/RG.2.2.14448.79360

Dudley, R., Platania, S., White, G., & Helfrich, D. (2012). *Rio Grande silvery minnow population estimation program results for 2011*. U.S. Bureau of Reclamation. https://doi.org/10.13140/RG.2.1.4201.3601

Dudley, R. K., Platania, S., & White, G. (2019). *Rio Grande silvery minnow population monitoring program during 2019* (p. 209). U.S. Bureau of Reclamation Albuquerque Office.

Ellegren, H. (2004). Microsatellites: Simple sequences with complex evolution. *Nature Reviews Genetics*, *5*, 435–445. https://doi.org/10.1038/nrg1348

Fischer, M. C., Rellstab, C., Leuzinger, M., Roumet, M., Gugerli, F., Shimizu, K. K., Holderegger, R., & Widmer, A. (2017). Estimating genomic diversity and population differentiation – An empirical comparison of microsatellite and SNP variation in *Arabidopsis halleri*. *BMC Genomics*, *18*(1), 1–15. https://doi.org/10.1186/s12864-016-3459-7

Forstmeier, W., Schielzeth, H., Mueller, J. C., Ellegren, H., & Kempenaers, B. (2012). Heterozygosity–fitness correlations in zebra finches: Microsatellite markers can be better than their reputation. *Molecular Ecology*, *21*(13), 3237–3249. https://doi.org/10.1111/j.1365-294X.2012.05593.x

Gilbert, K. J., & Whitlock, M. C. (2015). Evaluating methods for estimating local effective population size with and without migration. *Evolution*, *69*(8), 2154–2166. https://doi.org/10.1111/evo.12713

Gossieaux, P., Bernatchez, L., Sirois, P., & Garant, D. (2019). Impacts of stocking and its intensity on effective population size in brook Charr (*Salvelinus fontinalis*) populations. *Conservation Genetics*, *20*(4), 729–742. https://doi.org/10.1007/s10592-019-01168-2

Guillot, G., & Foll, M. (2009). Correcting for ascertainment bias in the inference of population structure. *Bioinformatics*, *25*(4), 552–554. https://doi.org/10.1093/bioinformatics/btn665

Guo, S. W., & Thompson, E. A. (1992). Performing the exact test of hardy-Weinberg proportion for multiple alleles. *Biometrics*, *48*(2), 361–372. https://doi.org/10.2307/2532296

Hedrick, P. W. (1999). Perspective: Highly variable loci and their interpretation in evolution and conservation. *Evolution*, *53*(2), 313–318. https://doi.org/10.1111/j.1558-5646.1999.tb03767.x

Hill, W. G. (1981). Estimation of effective population size from data on linkage disequilibrium. *Genetical Research*, *38*(3), 209–216. https://doi.org/10.1017/s0016672300020553

Hoban, S., Arntzen, J. A., Bruford, M. W., Godoy, J. A., Hoelzel, A., Segelbacher, G., Vilá, C., & Bertorelle, G. (2014). Comparative evaluation of potential indicators and temporal sampling protocols for

monitoring genetic erosion. *Evolutionary Applications*, *7*(9), 984–998. https://doi.org/10.1111/eva.12197

Hoffman, J. I., Simpson, F., David, P., Rijks, J. M., Kuiken, T., Thorne, M. A. S., Lacy, R. C., & Dasmahapatra, K. K. (2014). High-throughput sequencing reveals inbreeding depression in a natural population. *Proceedings of the National Academy of Sciences*, *111*(10), 3775–3780. https://doi.org/10.1073/pnas.1318945111

Horwitz, R. J., Keller, D. H., Overbeck, P. F., Platania, S. P., Dudley, R. K., & Carson, E. W. (2018). Age and growth of the Rio Grande silvery minnow, an endangered, short-lived cyprinid of the north American southwest. *Transactions of the American Fisheries Society*, *147*(2), 265–277. https://doi.org/10.1002/tafs.10012

Huisman, J., Kruuk, L. E., Ellis, P. A., Clutton-Brock, T., & Pemberton, J. M. (2016). Inbreeding depression across the lifespan in a wild mammal population. *Proceedings of the National Academy of Sciences*, *113*(13), 3585–3590. https://doi.org/10.1073/pnas.1518046113

Jombart, T., & Ahmed, I. (2011). Adegenet 1.3-1: New tools for the analysis of genome-wide SNP data. *Bioinformatics*, *27*(21), 3070–3071. https://doi.org/10.1093/bioinformatics/btr521

Jones, A. T., Ovenden, J. R., & Wang, Y. G. (2016). Improved confidence intervals for the linkage disequilibrium method for estimating effective population size. *Heredity*, *117*(4), 217–223. https://doi.org/10.1038/hdy.2016.19

Kardos, M., Åkesson, M., Fountain, T., Flagstad, Ø., Liberg, O., Olason, P., Sand, H., Wabakken, P., Wikenros, C., & Ellegren, H. (2018). Genomic consequences of intensive inbreeding in an isolated wolf population. *Nature Ecology & Evolution*, *2*(1), 124–131. https://doi.org/10.1038/s41559-017-0375-4

Kardos, M., Allendorf, F. W., & Luikart, G. (2014). Evaluating the role of inbreeding depression in heterozygosity-fitness correlations: How useful are tests for identity disequilibrium? *Molecular Ecology Resources*, *14*(3), 519–530. https://doi.org/10.1111/1755-0998.12193

Kassambara, A., & Kassambara, M. A. (2020). R Package *ggpubr*.

Keenan, K., McGinnity, P., Cross, T. F., Crozier, W. W., & Prodöhl, P. A. (2013). diveRsity: An R package for the estimation and exploration of population genetics parameters and their associated errors. *Methods in Ecology and Evolution*, *4*(8), 782–788. https://doi.org/10.1111/2041-210x.12067

Keller, M. C., Visscher, P. M., & Goddard, M. E. (2011). Quantification of inbreeding due to distant ancestors and its detection using dense single nucleotide polymorphism data. *Genetics*, *189*(1), 237–249. https://doi.org/10.1534/genetics.111.130922

Koelewijn, H. P., Pérez-Haro, M., Jansman, H. A. H., Boerwinkel, M. C., Bovenschen, J., Lammertsma, D. R., Niewold, F. J. J., & Kuiters, A. T. (2010). The reintroduction of the Eurasian otter (Lutra lutra) into The Netherlands: Hidden life revealed by noninvasive genetic monitoring. *Conservation Genetics*, *11*(2), 601–614. https://doi.org/10.1007/s10592-010-0051-6

Lehnert, S. J., DiBacco, C., Jeffery, N. W., Blakeslee, A. M. H., Isaksson, J., Roman, J., Wringe, B. F., Stanley, R. R. E., Matheson, K., McKenzie, C. H., Hamilton, L. C., & Bradbury, I. R. (2018). Temporal dynamics of genetic clines of invasive European green crab (*Carcinus maenas*) in eastern North America. *Evolutionary Applications*, *11*(9), 1656–1670. https://doi.org/10.1111/eva.12657

Lemopoulos, A., Prokkola, J. M., Uusi-Heikkilä, S., Vasemägi, A., Huusko, A., Hyvärinen, P., Koljonen, M., Koskiniemi, J., & Vainikka, A. (2019). Comparing RADseq and microsatellites for estimating genetic diversity and relatedness—Implications for brown trout conservation. *Ecology and Evolution*, *9*(4), 2106–2120. https://doi.org/10.1002/ece3.4905

Liaw, A., & Wiener, M. (2002). Classification and regression by random forest. *R news*, *2*, 18–22.

Ljungqvist, M., Åkesson, M., & Hansson, B. (2010). Do microsatellites reflect genome-wide genetic diversity in natural populations? A comment on Väli et al. (*2008*).

Lyubchich, V., Gel, Y. R., Brenning, A., Chu, C., Huang, X., Islambekov, U., Niamkova, P., Ofori-Boateng, D., Schaeffer, E. D., Vishwakarma, S., & Wang, X. (2022). Package 'funtimes'.

Mann, H. B. (1945). Nonparametric tests against trend. *Econometrica*, *13*(3), 245. https://doi.org/10.2307/1907187

Marandel, F., Charrier, G., Lamy, J. B., Le Cam, S., Lorance, P., & Trenkel, V. M. (2020). Estimating effective population size using RADseq: Effects of SNP selection and sample size. *Ecology and Evolution*, *10*(4), 1929–1937. https://doi.org/10.1002/ece3.6016

McLennan, E. A., Wright, B. R., Belov, K., Hogg, C. J., & Grueber, C. E. (2019). Too much of a good thing? Finding the most informative genetic data set to answer conservation questions. *Molecular Ecology Resources*, *19*(3), 659–671. https://doi.org/10.1111/1755-0998.12997

Meirmans, P. G. (2020). Genodive version 3.0: Easy-to-use software for the analysis of genetic data of diploids and polyploids. *Molecular Ecology Resources*, *20*(4), 1126–1131. https://doi.org/10.1111/1755-0998.13145

Meirmans, P. G., & Hedrick, P. W. (2011). Assessing population structure: F_{ST} and related measures. *Molecular Ecology Resources*, *11*(1), 5–18. https://doi.org/10.1111/j.1755-0998.2010.02927.x

Miller, J. M., & Coltman, D. W. (2014). Assessment of identity disequilibrium and its relation to empirical heterozygosity fitness correlations: A meta-analysis. *Molecular Ecology*, *23*(8), 1899–1909. https://doi.org/10.1111/mec.12707

Miller, J. M., Malenfant, R. M., David, P., Davis, C. S., Poissant, J., Hogg, J. T., Festa-Bianchet, M., & Coltman, D. W. (2014). Estimating genome-wide heterozygosity: Effects of demographic history and marker type. *Heredity*, *112*(3), 240–247. https://doi.org/10.1038/hdy.2013.99

Nei, M. (1987). *Molecular evolutionary genetics*. Columbia University Press.

Nei, M., & Tajima, F. (1981). Genetic drift and estimation of effective population size. *Genetics*, *98*(3), 625–640. https://doi.org/10.1093/genetics/98.3.625

Ohta, T., & Cockerham, C. C. (1974). Detrimental genes with partial selfing and effects on a neutral locus. *Genetics Research*, *23*(2), 191–200. https://doi.org/10.1017/S0016672300014816

O'Leary, S. J., Hollenbeck, C. M., Vega, R. R., & Portnoy, D. S. (2021). Disentangling complex genomic signals to understand population structure of an exploited, estuarine-dependent flatfish. *Ecology and Evolution*, *11*(19), 13415–13429. https://doi.org/10.1002/ece3.8064

Osborne, M. J., Benavides, M. A., Alò, D., & Turner, T. F. (2006). Genetic effects of hatchery propagation and rearing in the endangered Rio Grande silvery minnow, *Hybognathus amarus*. *Reviews in Fisheries Science*, *14*(1–2), 127–138. https://doi.org/10.1080/10641260500341544

Osborne, M. J., Benavides, M. A., & Turner, T. F. (2005). Genetic heterogeneity among pelagic egg samples and variance in reproductive success in an endangered freshwater fish, *Hybognathus amarus* (Cyprinidae). *Environmental Biology of Fishes*, *73*(4), 463–472. https://doi.org/10.1007/s10641-005-3215-3

Osborne, M. J., Carson, E. W., & Turner, T. F. (2012). Genetic monitoring and complex population dynamics: Insights from a 12-year study of the Rio Grande silvery minnow. *Evolutionary Applications*, *5*(6), 553–574. https://doi.org/10.1111/j.1752-4571.2011.00235.x

Osborne, M. J., Dowling, T. E., Scribner, K. T., & Turner, T. F. (2020). Wild at heart: Programs to diminish negative ecological and evolutionary effects of conservation hatcheries. *Biological Conservation*, *251*, 108768. https://doi.org/10.1016/j.biocon.2020.108768

Pflieger, W. L. (1980). Hybognathus nuchalis Agassiz, Central silvery minnow. In D. S. Lee, C. R. Gilbert, C. H. Hocutt, R. E. Jenkins, D. E. McAllister, & J. R. Stauffer Jr. (Eds.), *Atlas of North American freshwater fishes* (p. 177). North Carolina State Museum of Natural History.

Platania, S. P. (1993). *The fishes of the Rio Grande between Velarde and elephant Butte reservoir and their habitat associations* (Vol. *188*). New Mexico Department of Game and Fish, Santa Fe, and US Bureau of Reclamation (Albuquerque Projects Office).

Pohlert, T. (2020). Package "*trend*": Non-parametric trend tests and change-point detection vers. 1.1.4. R Package. 26.

R Core Team. (2020). *R: A language and environment for statistical computing*. R Foundation for Statistical Computing. https://www.R-project.org/

Rice, W. R. (1989). Analyzing tables of statistical tests. *Evolution*, *43*(1), 223–225. https://doi.org/10.2307/2409177

Robinson, S. P., Simmons, L. W., & Kennington, W. J. (2013). Estimating relatedness and inbreeding using molecular markers and pedigrees: The effect of demographic history. *Molecular Ecology*, *22*(23), 5779–5792. https://doi.org/10.1111/mec.12529

Rosner, B. (1983). Percentage points for a generalized ESD many-outlier procedure. *Technometrics*, *25*, 165–172.

Rousset, F. (2008). genepop'007: A complete re-implementation of the genepop software for windows and Linux. *Molecular Ecology Resources*, *8*(1), 103–106. https://doi.org/10.1111/j.1471-8286.2007.01931.x

RStudio Team. (2019). RStudio: Integrated development environment for R.

Russello, M. A., Waterhouse, M. D., Etter, P. D., & Johnson, E. A. (2015). From promise to practice: Pairing non-invasive sampling with genomics in conservation. *PeerJ*, *3*, e1106. https://doi.org/10.7717/peerj.1106

Schwartz, M., Luikart, G., & Waples, R. (2007). Genetic monitoring as a promising tool for conservation and management. *Trends in Ecology & Evolution*, *22*(1), 25–33. https://doi.org/10.1016/j.tree.2006.08.009

Sen, P. K. (1968). Estimates of the regression coefficient based on Kendall's tau. *Journal of the American Statistical Association*, *63*(324), 1379–1389. https://doi.org/10.1080/01621459.1968.10480934

Sin, S. Y. W., Hoover, B. A., Nevitt, G. A., & Edwards, S. V. (2021). Demographic history, not mating system, explains signatures of inbreeding and inbreeding depression in a large outbred population. *The American Naturalist*, *197*(6), 658–676. https://doi.org/10.1086/714079

Stoffel, M. A., Esser, M., Kardos, M., Humble, E., Nichols, H., David, P., & Hoffman, J. I. (2016). inbreedR: An R package for the analysis of inbreeding based on genetic markers. *Methods in Ecology and Evolution*, *7*(11), 1331–1339. https://doi.org/10.1111/2041-210X.12588

Sunde, J., Yıldırım, Y., Tibblin, P., & Forsman, A. (2020). Comparing the performance of microsatellites and RADseq in population genetic studies: Analysis of data for pike (*Esox lucius*) and a synthesis of previous studies. *Frontiers in Genetics*, *11*, 218. https://doi.org/10.3389/fgene.2020.00218

Szulkin, M., Bierne, N., & David, P. (2010). Heterozygosity-fitness correlations: A time for reappraisal. *Evolution*, *64*, 1202–1217. https://doi.org/10.1111/j.1558-5646.2010.00966.x

Townsend, S. M., & Jamieson, I. G. (2013). Molecular and pedigree measures of relatedness provide similar estimates of inbreeding depression in a bottlenecked population. *Journal of Evolutionary Biology*, *26*(4), 889–899. https://doi.org/10.1111/jeb.12109

Turner, T. F., Osborne, M. J., Moyer, G. R., Benavides, M. A., & Alò, D. (2006). Life history and environmental variation interact to determine effective population to census size ratio. *Proceedings of the Royal Society B: Biological Sciences*, *273*(1605), 3065–3073. https://doi.org/10.1098/rspb.2006.3677

Turner, T. F., Salter, L. A., & Gold, J. R. (2001). Temporal-method estimates of Ne from highly polymorphic loci. *Conservation Genetics*, *2*(4), 297–308. https://doi.org/10.1023/a:1012538611944

U.S. Fish and Wildlife Service. (1994). Endangered and threatened wildlife and plants: Final rule to list the Rio Grande silvery minnow as an endangered species. *Federal Register*, *59*, 36988–36995.

U.S. Fish and Wildlife Service. (2018a). Rio Grande silvery minnow genetics and propagation management plan, 2018 revision: Albuquerque, New Mexico.

U.S. Fish and Wildlife Service. (2018b). Rio Grande silvery minnow genetic management and captive propagation workgroup. Rio Grande silvery minnow annual augmentation plan, 2018–2022.

Väli, L., Einarsson, A., Waits, L., & Ellegren, H. (2008). To what extent do microsatellite markers reflect genome-wide genetic diversity in natural populations? *Molecular Ecology*, *17*(17), 3808–3817. https://doi.org/10.1111/j.1365-294x.2008.03876.x

Vendrami, D. L. J., de Noia, M., Telesca, L., Brodte, E., & Hoffman, J. I. (2020). Genome-wide insights into introgression and its consequences for genome-wide heterozygosity in the *Mytilus* species complex across Europe. *Evolutionary Applications*, *13*(8), 2130–2142. https://doi.org/10.1111/eva.12974

Wang, J. (2021). EMIBD9 software. https://www.zsl.org/science/software/emibd9

Wang, L., Akritas, M. G., & Van Keilegom, I. (2008). An ANOVA-type nonparametric diagnostic test for heteroscedastic regression models. *Journal of Nonparametric Statistics*, *20*(5), 365–382.

Waples, R. S. (1989). A generalized approach for estimating effective population size from temporal changes in allele frequency. *Genetics*, *121*(2), 379–391. https://doi.org/10.1093/genetics/121.2.379

Waples, R. S. (2005). Genetic estimates of contemporary effective population size: To what time periods do the estimates apply? *Molecular Ecology*, *14*(11), 3335–3352. https://doi.org/10.1111/j.1365-294x.2005.02673.x

Waples, R. S. (2015). Testing for hardy–Weinberg proportions: Have we lost the plot? *Journal of Heredity*, *106*(1), 1–19. https://doi.org/10.1093/jhered/esu062

Waples, R. S., & Do, C. (2010). Linkage disequilibrium estimates of contemporary NeV using highly variable genetic markers: A largely untapped resource for applied conservation and evolution. *Evolutionary Applications*, *3*(3), 244–262. https://doi.org/10.1111/j.1752-4571.2009.00104.x

Willis, S. C., Hollenbeck, C. M., Puritz, J. B., Gold, J. R., & Portnoy, D. S. (2017). Haplotyping RAD loci: An efficient method to filter paralogs and account for physical linkage. *Molecular Ecology Resources*, *17*(5), 955–965. https://doi.org/10.1111/1755-0998.12647

Wright, S. (1950). Genetical structure of populations. *Nature*, *166*, 247–249.

Yackulic, C., Archdeacon, T., Valdez, R., Hobbs, M., Porter, M., Lusk, J., Tanner, A., Gonzales, E., Lee, D., & Haggerty, G. (2022). Quantifying flow and nonflow management impacts on an endangered fish by integrating, data, research, and expert opinion. *Ecosphere*, *13*(9), e4240. https://doi.org/10.1002/ecs2.4240

Zimmerman, S. J., Aldridge, C. L., & Oyler-McCance, S. J. (2020). An empirical comparison of population genetic analyses using microsatellite and SNP data for a species of conservation concern. *BMC Genomics*, *21*(1), 1–16. https://doi.org/10.1186/s12864-020-06783-9

SUPPORTING INFORMATION

Additional supporting information can be found online in the Supporting Information section at the end of this article.

How to cite this article: Osborne, M. J., Caeiro-Dias, G., & Turner, T. F. (2023). Transitioning from microsatellites to SNP-based microhaplotypes in genetic monitoring programmes: Lessons from paired data spanning 20 years. *Molecular Ecology*, *32*, 316–334. https://doi.org/10.1111/mec.16760